

---

# Learning Partially Known Stochastic Dynamics with Empirical PAC Bayes

---

Manuel Haußmann<sup>1\*</sup>Sebastian Gerwinn<sup>2\*</sup>Andreas Look<sup>2</sup>Barbara Rakitsch<sup>2</sup>Melih Kandemir<sup>2</sup><sup>1</sup>HCI/TWR, Heidelberg University, Germany

manuel.haussmann@iwr.uni-heidelberg.de

<sup>2</sup>Bosch Center for Artificial Intelligence, Renningen, Germany

firstname.lastname@de.bosch.com

## Abstract

We propose a novel scheme for fitting heavily parameterized non-linear stochastic differential equations (SDEs). We assign a prior on the parameters of the SDE drift and diffusion functions to achieve a Bayesian model. We then infer this model using the well-known local reparameterized trick for the first time for empirical Bayes, i.e. to integrate out the SDE parameters. The model is then fit by maximizing the likelihood of the resultant marginal with respect to a potentially large number of hyperparameters, which prohibits stable training. As the prior parameters are marginalized, the model also no longer provides a principled means to incorporate prior knowledge. We overcome both of these drawbacks by deriving a training loss that comprises the marginal likelihood of the predictor and a PAC-Bayesian complexity penalty. We observe on synthetic as well as real-world time series prediction tasks that our method provides an improved model fit accompanied with favorable extrapolation properties when provided a partial description of the environment dynamics. Hence, we view the outcome as a promising attempt for building cutting-edge hybrid learning systems that effectively combine first-principle physics and data-driven approaches.

## 1 Introduction

Modeling obvious regularities in physical phenomena is easy, excelling at simulating their behavior is hard. As the standard practice of applied sciences, domain experts model dynamical environments with differential equation systems. It is often the case that a small set of variables in straightforward relationships is sufficient to hit a Pareto frontier with reasonable effort and expertise. However, pushing a model beyond this frontier towards high fidelity either requires an unreasonably amount of time from a dedicated expert or demands unaffordable computational resources.

We address the necessity to bridge the gap between interpretable but incomplete domain expert solutions and highly accurate but black-box data scientist solutions as a non-linear system identification problem with partially known system characteristics. We assume to have access to a differential equation system that describes the dynamics of the target environment with low fidelity, e.g. by describing the vector field on a reduced dimensionality, by ignoring detailed models of some system

---

\*equal contribution

components, or by avoiding certain dependencies for computational feasibility. We incorporate the ODE system provided by the domain expert into a non-linear system identification engine, which we choose to be a *Bayesian Neural Stochastic Differential Equation* (BNSDE) to cover a large scope of systems, resulting in a *hybrid model* describing the complex system dynamics.

We propose a new algorithm for stable and effective training of a hybrid BNSDE that combines the strengths of two statistical approaches: i) Bayesian model selection (Kass and Raftery, 1995), and ii) Probably Approximately Correct (PAC) Bayesian training (McAllester, 1999; Seeger, 2002). We improve on the previously proven theoretical links between these two approaches (Germain et al., 2016) by showing that it is possible to benefit from both of them *during* training time by choosing the risk definitions of the PAC framework suitably. The bound we develop admits the marginal likelihood of a BNSDE as an additive term to model complexity that brings together effective training by directly optimizing the predictive distribution (the end product of interest) and complexity penalization. While being rather loose for providing generalization guarantees, this bound can serve as a training objective that follows tied gradient steps to a tighter PAC bound.

We evaluate our method on challenging time-series data sets. Our method exhibits great success in exploiting coarse descriptions of true underlying dynamics into a consistent increase in forecasting accuracy. We also observe it to deliver state-of-the-art performance on a real-world time series prediction data set, outperforming black-box system identification approaches (Chen et al., 2018; Hegde et al., 2019; Look and Kandemir, 2019) and alternative hybridization schemes incorporating second-order Newtonian mechanics (Yildiz et al., 2019).

## 2 Bayesian Stochastic Differential Equations

Given a time series  $\mathbf{Y} = \{\mathbf{y}_1, \dots, \mathbf{y}_K\}$  of length  $K$  consisting of  $D$ -dimensional observations  $\mathbf{y}_k$  collected from a dynamical environment at potentially irregular time points  $\mathbf{t} = \{t_1, t_2, \dots, t_K\}$ , we model the environment dynamics with a stochastic differential equation (SDE) as

$$\theta_f \sim p_{\phi_f}(\theta_f), \quad \theta_G \sim p_{\phi_G}(\theta_G), \quad (1)$$

$$d\mathbf{h}_t | \theta_f, \theta_G \sim f_{\theta_f}(\mathbf{h}_t, t)dt + G_{\theta_G}(\mathbf{h}_t, t)d\beta_t, \quad (2)$$

$$\mathbf{z}_k | \mathbf{h}_k \sim p_{\psi}(\mathbf{z}_k | \mathbf{h}_k), \quad \mathbf{y}_k | \mathbf{z}_k \sim p(\mathbf{y}_k | \mathbf{z}_k), \quad \forall t_k \in \mathbf{t}, \quad (3)$$

where  $f_{\theta_f}(\cdot, \cdot) : \mathbb{R}^P \times \mathbb{R}_+ \rightarrow \mathbb{R}^P$  is an arbitrary non-linear drift function parameterized by  $\theta_f$  governing the vector field of a latent  $\mathbf{h}_t \in \mathbb{R}^P$  with potentially  $P \ll D$ , which satisfies  $L$ -Lipschitz continuity constraints for some  $0 < L < \infty$ . The non-linear diffusion dynamics satisfying the same continuity constraints are governed via the matrix-valued function  $G_{\theta_G}(\cdot, \cdot) : \mathbb{R}^P \times \mathbb{R}_+ \rightarrow \mathbb{R}^{P \times P}$  parameterized by  $\theta_G$  with potentially  $\theta_f \cap \theta_G \neq \emptyset$ . The diffusion term also contains  $\beta_t$ , which follows Brownian motion dynamics, for any time step  $\Delta t$ , it follows  $\beta_t \sim \mathcal{N}(0, \Delta t)$ . We assume the latent state  $\mathbf{h}_t$  to be mapped to a potentially higher dimensional observation space  $\mathbf{z}_t$  via a density function  $p_{\psi}(\mathbf{z}_t | \mathbf{h}_t)$  parameterized by  $\psi$ , while  $p(\mathbf{y}_t | \mathbf{z}_t)$  is a simple parameter-free likelihood function (e.g., CMU-dataset, Table 2, Appendix D). In case  $f_{\theta_f}$  and  $G_{\theta_G}$  are modeled with neural nets of arbitrary architectures, we refer to this model as a *Bayesian Neural SDE* (BNSDE).

The resultant system has two main sources of uncertainty in the latent space: i) the prior distributions ( $p_{\phi_f}(\theta_f), p(\theta_G)$ ) and ii) the Brownian motion. While the latter is meant to capture the inherent uncertainty in the dynamical environment the former accounts for model uncertainty, which could be vital especially in system identification as uncertainty accumulates through time steps.

Solving the SDE system in (2) for a time interval  $[0, T]$  and fixed  $\theta_f, \theta_G$  requires computing integrals of the form  $\int_0^T d\mathbf{h}_t = \int_0^T f_{\theta_f}(\mathbf{h}_t, t)dt + \int_0^T G_{\theta_G}(\mathbf{h}_t, t)d\beta_t$ . Since both integrals cannot be computed in closed-form (see Appendix A), we discretize the solution and approximate its transition densities. For the dynamical system, a time series  $\mathbf{Y}$  observed at time indices  $\mathbf{t}$  can be approximated by a discrete-time probabilistic model such as the Euler-Maruyama discretization:

$$\begin{aligned} \theta_f &\sim p_{\phi_f}(\theta_f), \quad \theta_G \sim p_{\phi_G}(\theta_G), \quad \mathbf{h}_0 \sim p(\mathbf{h}_0), \\ \mathbf{h}_{k+1} | \mathbf{h}_k, \theta_f, \theta_G &\sim \mathcal{N}\left(\mathbf{h}_{k+1} | \mathbf{h}_k + f_{\theta_f}(\mathbf{h}_k, t_k)\Delta t_k, \mathbf{J}_k \Delta t_k\right), \\ \mathbf{Y}, \mathbf{Z} | \mathbf{H} &\sim \prod_{k=1}^K \left[ p(\mathbf{y}_k | \mathbf{z}_k) p_{\psi}(\mathbf{z}_k | \mathbf{h}_k) \right], \end{aligned} \quad (4)$$

with  $\mathbf{J}_k = G_{\theta_G}(\mathbf{h}_k, k)G_{\theta_G}(\mathbf{h}_k, k)^T$ ,  $\Delta t_k = t_{k+1} - t_k$ ,  $\theta = (\theta_f, \theta_G)$ ,  $\mathbf{H} = \{\mathbf{h}_1, \dots, \mathbf{h}_K\}$ , and  $\mathbf{Z} = \{\mathbf{z}_1, \dots, \mathbf{z}_K\}$ . The distribution  $p(\mathbf{h}_0)$  is defined on the initial latent state.

### 3 Model Learning and Local Reparameterization Trick

The mainstream approach for the inference of such groups of variables is to approximate  $p(\theta_f, \theta_G, \mathbf{H}, \mathbf{Z}|\mathbf{Y})$  during training, integrate out  $\mathbf{H}$  and  $\mathbf{Z}$ , and then use the approximate posterior distribution on the dynamics  $p(\theta_f, \theta_G|\mathbf{Y})$  for prediction. Often the posterior  $p(\theta_f, \theta_G|\mathbf{Y})$  is intractable, hence approximation techniques such as variational inference or Markov Chain Monte Carlo (MCMC) are used. Embedding an MCMC method into an SDE inference scheme is not straightforward due to the high estimator variance induced by the samples taken directly on global latent variables  $\theta_f$  and  $\theta_G$  (Look and Kandemir, 2019). AS for variational inference, further simplifying assumptions on the posterior are made to assure closed-form calculation of transition densities (Archambeau et al., 2008).

**Learning via model selection.** This approach instead suggests marginalizing out all latent variables, comparing the marginal likelihoods of all possible hypotheses, and choosing the one providing the highest response (Kass and Raftery, 1995). A model is trained on data by choosing the hyperparameters that maximize the marginal likelihood

$$\arg \max_{\phi_f, \phi_G, \psi} \log \left[ \int \int p(\mathbf{Y}|\mathbf{Z})p_\psi(\mathbf{Z}|\mathbf{H})p(\mathbf{H}|\theta_f, \theta_G)p_{\phi_f}(\theta_f)p_{\phi_G}(\theta_G)d\mathbf{Z}d\mathbf{H}d\theta_f d\theta_G \right], \quad (5)$$

by-passing the posterior inference step on latent variables, known as *Empirical Bayes* (Efron, 2012). Despite not explicitly modeling the uncertainty on the hyperparameters  $\phi_f$ ,  $\phi_G$ , and  $\psi$ , the key advantage of empirical Bayes is that it directly models the marginal predictive distribution requiring fewer approximation steps until a tractable solution. With its appealing computational requirements, direct predictive distribution modeling has been investigated in the recent literature and applied successfully in uncertainty-aware tasks (Sensoy et al., 2018; Malinin and Gales, 2018; Garnelo et al., 2018). Due to its inherent suitability to the implicit nature of stochastic processes defined as nonlinear SDEs, we adopt this approach for inference and demonstrate its effectiveness in our experiments.

**Empirical Bayes for SDEs.** Marginalizing  $\theta_f$  and  $\theta_G$  in (5) is an intractable problem for most modeling choices in practice. However, we can marginalize over  $\theta$  by MC integration without constructing Markov chains on the global parameters. Instead, we directly sample from the prior and use the marginal log-likelihood as the objective function to tune the hyperparameters:

$$\forall s = 1, \dots, S : \quad \theta_f^s \sim p_{\phi_f}(\theta_f), \quad \theta_G^s \sim p_{\phi_G}(\theta_G), \quad \mathbf{H}^s \sim p(\mathbf{H}|\theta_f^s, \theta_G^s),$$

$$\phi_f^*, \phi_G^*, \psi^* = \arg \max_{\phi_f, \phi_G, \psi} \log \left[ \frac{1}{S} \sum_{s=1}^S p(\mathbf{Y}|\mathbf{Z}^s)p_\psi(\mathbf{Z}^s|\mathbf{H}^s) \right], \quad (6)$$

where  $S$  is the Monte Carlo sample count per parameter set and  $p(\mathbf{H}|\theta_f^s, \theta_G^s)$  is the distribution imposed by the SDE in (2) for the subsumed discretization  $\mathbf{t}$ . A draw from this distribution can be taken following the generative process in (4) with the sampled parameters  $\theta_f^s$  and  $\theta_G^s$ . In the BNSDE case, gradients need to be passed on the parameters  $\phi$  of the distributions  $p_\phi(\theta)$  used to take samples, which can simply be done by reparameterization, i.e.  $\varepsilon \sim p(\varepsilon)$ ,  $\theta = g_\phi(\varepsilon)$ . We lower the estimator variance further using the *local reparameterization trick* (Kingma et al., 2015). Instead of sampling the weights  $\theta$  directly, this translates into local noise  $p(v_{mk})$  attached to every neuron  $m$  and independent across time points  $t_k$ . While the local reparameterization trick has been used earlier in state-space models for variational inference (Doerr et al., 2018), for the first time we apply it to empirical Bayes as well as BNSDE inference. Placing normal priors on weights, we get the following distribution on the linear  $M'$  dimensional pre-activation outputs  $\mathbf{v}_k$  of a layer:

$$v_{m'k} \sim \mathcal{N}\left(v_{m'k} \mid \sum_{m=1}^M \mu_{mm'} u_{mk}, \sum_{m=1}^M \sigma_{mm'}^2 u_{mk}^2\right),$$

where  $u_{mk}$  is the  $M$  dimensional input to the layer and  $\mu_{mm'}, \sigma_{mm'}^2$  are the mean/variance hyperparameters. Then we generate latent state samples  $\mathbf{H}^s = \mathbf{h}_k^s, k = 1, \dots, K$  by

$$\varepsilon_k^s \sim p(\varepsilon), \quad \tilde{\varepsilon}_k^s \sim p(\tilde{\varepsilon}), \quad \forall s, k \in \{1, \dots, S\} \times \{1, \dots, K\},$$

$$\mathbf{h}_k^s \sim p(\mathbf{h}_k^s | f_k^s = g_{\phi_f}(\varepsilon_k^s, \mathbf{h}_{k-1}^s), G_k^s = g_{\phi_G}(\tilde{\varepsilon}_k^s, \mathbf{h}_{k-1}^s)),$$

which are then used within the training procedure (6), leading to a reduction in the variance of our marginal likelihood estimate which in turn leads to a faster convergence when optimizing for the hyperparameters  $\phi_f, \phi_G, \psi$ .

## 4 Hybrid SDE Learning with Empirical PAC Bayes

We thus far have modeled a time series as a black-box BNSDE. In many real-world applications, however, we have access to a coarse and incomplete description of the environment dynamics. For instance, the dynamics of a three-dimensional volume might be modeled as a flow through a single point, such as the center of mass. Alternatively, a model on a subset of the system components might be provided. Let us assume that this prior knowledge is available as an ODE,

$$d\mathbf{h}_t = r_\xi(\mathbf{h}_t, t)dt, \quad (7)$$

where  $r_\xi(\cdot, \cdot) : \mathbb{R}^P \times \mathbb{R}_+ \rightarrow \mathbb{R}$  is an arbitrary non-linear function parameterized by  $\xi$ .

We incorporate these known dynamics into the system adding them to the drift

$$\theta_f, \theta_G \sim q_{\phi_f}, q_{\phi_G}, \quad \mathbf{h}_t = (f_{\theta_f}(\mathbf{h}_t, t) + \gamma \circ r_\xi(\mathbf{h}_t, t))dt + G_{\theta_G}(\mathbf{h}_t, t)d\beta_t, \quad \mathbf{z}_t | \mathbf{h}_t \sim p_\psi, \quad (8)$$

which can be viewed as a hybrid stochastic differential equation with the free parameter vector  $\gamma \in [0, 1]^P$  governing the relative importance of prior knowledge on the learning problem and  $\circ$  referring to element-wise multiplication. Although we specified (7) within the same dimensional state space as (8), the free parameter  $\gamma$  allows us to provide only partial information, setting  $\gamma_p = 0$  for the dimension  $p$  with no information.

The new SDE representing the prior knowledge of the dynamics is then given as

$$d\mathbf{h}_t = (\gamma \circ r_\xi(\mathbf{h}_t, t))dt + G_{\theta_G}(\mathbf{h}_t, t)d\beta_t, \quad (9)$$

which we will use to set a reference distribution for complexity penalization during PAC training of our hybrid SDE. Although the above SDEs have continuous time-solutions (see App. A), we use a discrete time approximation, obtained via application of the Euler-Maruyama method. This can be described by finite-dimensional distribution of the two stochastic processes. More precisely, for any time horizon  $T > 0$  and discretization  $\{t_i | i = 1 \dots, n_T\}$ , there is finite dimensional distribution in terms of a density of  $\mathbf{h}_{0 \rightarrow T} := \{\mathbf{h}_{t_i} | i = 1, \dots, n_T\}$ . As such a construction is feasible for any discretization, we omit the dependence on a particular discretization and denote the distribution of the stochastic process of the SDE in (8) and (9) on the latent space as  $p_{\text{hyb}}(\mathbf{h}_{0 \rightarrow T} | \theta_f, \theta_G)$  and  $p_{\text{pri}}(\mathbf{h}_{0 \rightarrow T} | \theta_G)$ . Additionally, we have for both SDEs

$$\theta_f \sim p(\theta_f), \quad \theta_G \sim p(\theta_G), \quad \mathbf{z}_t | \mathbf{h}_t \sim p_\psi(\mathbf{z}_t | \mathbf{h}_t),$$

where distributions without tunable hyperparameters are placed on  $\theta_f$  and  $\theta_G$ . Note also that the hybrid and the prior SDEs share the same diffusion and observation model. Finally, we construct the distribution over hypotheses  $(\mathbf{z}_{0 \rightarrow T}, \mathbf{h}_{0 \rightarrow T}, \theta_f, \theta_G)$  via the hybrid process joint

$$Q_{0 \rightarrow T}(\mathbf{z}_{0 \rightarrow T}, \mathbf{h}_{0 \rightarrow T}, \theta_f, \theta_G) = p_\psi(\mathbf{z}_{0 \rightarrow T} | \mathbf{h}_{0 \rightarrow T})p_{\text{hyb}}(\mathbf{h}_{0 \rightarrow T} | \theta_f, \theta_G)q_{\phi_f}(\theta_f)q_{\phi_G}(\theta_G),$$

and the prior distribution via the prior process joint

$$P_{0 \rightarrow T}(\mathbf{z}_{0 \rightarrow T}, \mathbf{h}_{0 \rightarrow T}, \theta_f, \theta_G) = p_\psi(\mathbf{z}_{0 \rightarrow T} | \mathbf{h}_{0 \rightarrow T})p_{\text{pri}}(\mathbf{h}_{0 \rightarrow T} | \theta_G)p(\theta_f)p(\theta_G).$$

Above,  $p_\psi(\mathbf{z}_{0 \rightarrow T} | \mathbf{h}_{0 \rightarrow T})$  stands for the probability density of the observation model evaluated at every instant across the dense time interval  $[0, T]$ . Even though the definition of this object requires rigor, the downstream operations in the development of the training objective are agnostic to its representation in the continuous-time domain. Now we develop a divergence between the two process marginals straightforwardly extending the proof of (Archambeau et al., 2008). Note, that the following Lemma holds for any choice of hyper-parameters  $\psi_f, \psi_r$  determining the hypothesis class  $Q_{0 \rightarrow T}$ , which will be later used in the upcoming PAC bound.

**Lemma 1.** For the process distributions  $Q_{0 \rightarrow T}$  and  $P_{0 \rightarrow T}$ , the following property holds

$$D_{KL}(Q_{0 \rightarrow T} || P_{0 \rightarrow T}) = \frac{1}{2} \int_0^T \mathbb{E}_{Q_{0 \rightarrow T}} \left[ f_{\theta_f}(\mathbf{h}_t, t)^T \mathbf{J}_t^{-1} f_{\theta_f}(\mathbf{h}_t, t) \right] dt \\ + D_{KL}(q(\theta_f) || p(\theta_f)) + D_{KL}(q(\theta_G) || p(\theta_G))$$

for some  $T > 0$ , where  $\mathbf{J}_t = G_{\theta_G}(\mathbf{h}_t, t) G_{\theta_G}(\mathbf{h}_t, t)^T$ .

This KL term is not a function of the prior drift parameters  $\xi$ , unlike the construction in (de G. Matthews et al., 2016) which was later extended to learnable PAC priors by (Reeb et al., 2018) at the expense of loosening the bound as a learnable hyperparameter precision. Our construction is immune to such complications, hence,  $\xi$  can be identified jointly with  $\phi_f$  and  $\phi_G$  if desired. Below, we arrive at a stably trainable hybrid dynamics model by complementing the marginal likelihood objective of (5) with a penalty term derived from learning-theoretic first principles. The proofs for the preceding Lemma and the following three theorems can be found in the appendix.

**Theorem 1.** Let  $p(\mathbf{y}_t | \mathbf{z}_t)$  be uniformly bounded likelihood function with density  $p(\mathbf{y}_t | \mathbf{z}_t)$  everywhere,  $p_\psi(\mathbf{z}_t | \mathbf{h}_t)$  be an also bounded observation model, and  $Q_{0 \rightarrow T}$  and  $P_{0 \rightarrow T}$  be the joints of the posterior and prior stochastic processes defined on the hypothesis class of the learning task, respectively. Define the true risk of a draw from  $Q_{0 \rightarrow T}$  on an i.i.d. sample  $\mathbf{Y} = \{\mathbf{y}_1, \dots, \mathbf{y}_K\}$  at discrete and potentially irregular time points  $t_1, \dots, t_K$  drawn from an unknown ground-truth stochastic process  $G(t)$  as the expected model misfit as on the sample as defined via the following risk over hypotheses  $Q = \mathbf{z}_{0 \rightarrow T}, \mathbf{h}_{0 \rightarrow T}, \theta_f, \theta_G$  for an arbitrary, but bounded choice of  $q(\theta_G)q(\theta_f)$

$$R(Q) = -\mathbb{E}_{\mathbf{Y} \sim G(t)} \left[ \prod_{k=1}^K \left[ p(\mathbf{y}_k | \mathbf{z}_k) p(\mathbf{z}_k | \mathbf{h}_k) q(\mathbf{h}_k | \mathbf{h}_{k-1}, \theta_f, \theta_G) \right] p(\mathbf{h}_0) q(\theta_f) q(\theta_G) \right], \quad (10)$$

for time horizon  $T > 0$  and the corresponding empirical risk on a data set  $\mathcal{D} = \{\mathbf{Y}_1, \dots, \mathbf{Y}_N\}$  as

$$R_{\mathcal{D}}(Q) = -\frac{1}{N} \sum_{n=1}^N \left[ \prod_{k=1}^K \left[ p(\mathbf{y}_k^n | \mathbf{z}_k^n) p(\mathbf{z}_k^n | \mathbf{h}_k^n) q(\mathbf{h}_k^n | \mathbf{h}_{k-1}^n, \theta_f, \theta_G) \right] p(\mathbf{h}_0^n) q(\theta_f) q(\theta_G) \right]. \quad (11)$$

Then the expected true risk is bounded above by the marginal negative log-likelihood of the predictor and a complexity functional as

$$\mathbb{E}_{Q_{0 \rightarrow T}} [R(Q)] \leq \mathbb{E}_{Q_{0 \rightarrow T}} [R_{\mathcal{D}}(Q)] + \mathcal{C}_\delta(Q_{0 \rightarrow T}, P_{0 \rightarrow T}), \quad (12) \\ \leq -\frac{1}{SN} \sum_{n=1}^N \sum_{s=1}^S \left\{ \left[ \sum_{k=1}^K \ln \left( p(\mathbf{y}_k^n | \mathbf{z}_k^{s,n}) p(\mathbf{z}_k^{s,n} | \mathbf{h}_k^{s,n}) q(\mathbf{h}_k^{s,n} | \mathbf{h}_{k-1}^{s,n}, \theta_f^{s,n}, \theta_G^{s,n}) p(\mathbf{h}_0^{s,n}) \right) \right] \right. \\ \left. + \ln q(\theta_f^{s,n}) + \ln q(\theta_G^{s,n}) \right\} + \mathcal{C}_{\delta/2}(Q_{0 \rightarrow T}, P_{0 \rightarrow T}) + \sqrt{\frac{\ln(2N/\delta)}{2S}} + K \ln \bar{B}, \quad (13)$$

where  $\bar{B} := \max_{\mathbf{y}_k, \mathbf{h}_k, \theta_f, \theta_G} p(\mathbf{y}_k, \mathbf{h}_k | \theta_f, \theta_G) q(\theta_f) q(\theta_G)$  is the uniform bound,  $S$  is the sample count taken independently for each observed sequence, and the complexity functional is given as

$$\mathcal{C}_\delta(Q_{0 \rightarrow T}, P_{0 \rightarrow T}) := \sqrt{1/(2N)} \sqrt{D_{KL}(Q_{0 \rightarrow T} || P_{0 \rightarrow T}) + \ln(2\sqrt{N}) - \ln(\delta/2)}$$

with  $D_{KL}(Q_{0 \rightarrow T} || P_{0 \rightarrow T})$  as in Lemma 1 for some  $\delta > 0$ .

Although we require i.i.d. observations of time-series, we can in practice use mini-batches of trajectories provided that the batches are sufficiently far apart such that they become independent. Remarkably, the term  $\mathbb{E}_{Q_{0 \rightarrow T}} [R_{\mathcal{D}}(Q)]$  in (12) does not correspond to Empirical Bayes, as it averages over single sequence likelihoods. When the  $\ln(\cdot)$  function is placed into its summands, the first term of (13) is a sample approximation to the marginal data log-likelihood  $\ln p(\mathbf{Y}_1, \dots, \mathbf{Y}_N)$ . Maximizing it subject to the hyperparameters is Empirical Bayes. We adopt this bound as our training objective, where the constant terms ( $K \ln(\bar{B}) + \sqrt{\ln(2N/\delta)/(2S)}$ ) can be ignored. Training this objective also tightens the PAC bound as we show with the following theorem.

---

**Algorithm 1:** E-PAC-Bayes-Hybrid Loss Construction

---

**Input:** observed set of trajectories  $\mathcal{D} = \{\mathbf{Y}_1, \dots, \mathbf{Y}_N\}$  s.t.  $\mathbf{Y}_n = \{\mathbf{y}_1^n, \dots, \mathbf{y}_K^n\}$ , prior drift  $r(\cdot, \cdot)$ , drift  $f_{\theta_f}(\cdot, \cdot)$  and diffusion  $G_{\theta_G}(\cdot, \cdot)$  functions as BNNs, observation model  $p_\psi(\mathbf{z}_t | \mathbf{h}_t)$ , weight posteriors  $q_{\phi_f}(\theta_f)$ ,  $q_{\phi_G}(\theta_G)$  and priors  $p(\theta_f)$ ,  $p(\theta_G)$ , horizon  $K$ , no. samples  $S$

**Output:** training objective loss

loglik  $\leftarrow$  0, kl  $\leftarrow$  0 // initialize log-likelihood and kl term

**for**  $n, s \in \{1, \dots, N\} \times \{1, \dots, S\}$  **do**

$\mathbf{h}_0^{s,n} \sim p(\mathbf{h}_0)$ ;  $\theta_f^{s,n} \sim q_{\phi_f}$ ,  $\theta_G^{s,n} \sim q_{\phi_G}$

**for**  $k \leftarrow 1 : K$  **do**

$f_k^{s,n} \leftarrow f_{\theta_f^{s,n}}(\mathbf{h}_{k-1}^{s,n}, t_{k-1})$

$r_k^n \leftarrow r_{\theta_G^{s,n}}(\mathbf{h}_{k-1}^{s,n}, t_{k-1})$

$L_k^{s,n} \leftarrow G_{\theta_G^{s,n}}(\mathbf{h}_{k-1}^{s,n}, t_{k-1})$

$\Delta t_k \leftarrow t_k - t_{k-1}$

$\beta_k^{s,n} \sim \mathcal{N}(0, \Delta t_k \mathbf{I})$ ,

$\mathbf{h}_k^{s,n} \leftarrow \mathbf{h}_{k-1}^{s,n} + (f_k^{s,n} + \gamma r_k^{s,n}) \Delta t_k + L_k^{s,n} \beta_k^{s,n}$

$\widehat{\mathbf{z}}_k^{s,n} \sim p_\psi(\mathbf{z}_k^{s,n} | \mathbf{h}_k^{s,n})$

loglik  $\leftarrow$  loglik +  $\frac{1}{SN} \ln p(\mathbf{y}_k^n | \widehat{\mathbf{z}}_k^{s,n})$ ;

kl  $\leftarrow$  kl +  $\frac{1}{2S} f_k^{s,n T} (L_k^{s,n} L_k^{s,n T})^{-1} f_k^{s,n} \Delta t_k$

**end for**

**end for**

kl  $\leftarrow$  kl +  $D_{KL}(q_{\phi_f}(\theta_f) q_{\phi_G}(\theta_G) \| p(\theta_f) p(\theta_G))$

loss  $\leftarrow$  -loglik +  $\sqrt{(\text{kl} + \ln(4\sqrt{N}/\delta)) / (2N)}$

**return** loss

---

**Theorem 2.** For Lipschitz-continuous risk and likelihood, a gradient step that reduces (13) also tightens the PAC bound in (12).

Hence, gradient-based training of (13) also performs PAC learning. Placing the hybrid SDE into this training objective, we arrive at the generically applicable procedure given in Algorithm 1 for its construction. One can pass the gradients on the hyperparameters  $(\phi_f, \phi_G, \psi)$  through this objective and train on any observed set of trajectories.

Our sample-driven method couples naturally with the sample-driven Euler Maruyama (EM) approximation and inherits its convergence properties. Below we show strong convergence to the true solution with shrinking step size that follows as a simple extension of the plain EM proof (Kloeden and Platen, 2011), also implying weak convergence.

**Theorem 3 (strong convergence).** Let  $\mathbf{h}_t^\theta$  be an Itô process as in (2) with drift and diffusion parameters  $\theta = \{\theta_f \cup \theta_G\}$  and its Euler-Maruyama approximation  $\tilde{\mathbf{h}}_t^\theta$  as in (4) for some regular step size  $\Delta t > 0$ . For some coefficient  $R > 0$  and any  $T > 0$ , the inequality below holds

$$\mathbb{E} \left[ \sup_{0 \leq t \leq T} \left| \mathbb{E}_\theta[\mathbf{h}_t^\theta] - \frac{1}{S} \sum_{s=1}^S \tilde{\mathbf{h}}_t^{\theta^{(s)}} \right| \right] \leq R \Delta t^{1/2},$$

as  $S \rightarrow \infty$  where  $\{\theta^{(s)} \sim p_\phi(\theta) | s = 1, \dots, S\}$  are i.i.d. draws from a prior  $p_\phi(\theta)$ .

## 5 Relation to Closest Prior Art

**Empirical Bayes as PAC Learning.** Germain et al. (2016) propose a learnable PAC bound that provides generalization guarantees as a function of a marginal log-likelihood. Our method differs from this work in two main lines. First, Germain et al. (2016) define risk as  $-\log p(\mathbf{Y} | \mathbf{Z}) \in (-\infty, +\infty)$  and compensate for the unboundedness of by either truncating the support of the likelihood function or introducing assumptions the data distribution, such as sub-Gaussian or sub-gamma. Contrarily, our risk defined in (10) assumes uniformly boundedness, yet can be plugged in a PAC bound without



further restrictions on the data. Second, [Germain et al. \(2016\)](#)’s PAC bound is an unparameterized rescaling of the marginal log-likelihood. Hence, it is not linked to capacity penalizer, which can be used at *training time* for regularization. As applying this method to hybrid sequence modeling boils down to performing plain empirical Bayes, we also compare to this alternative in our experiments.

**Empirical Bayes as PAC Learning.** [Hegde et al. \(2019\)](#) model the dynamics of the activation maps of a *feed-forward* learner by the predictive distribution of a GP. This method allocates the mean of a GP as the drift and covariance as the diffusion. It infers the resultant model using variational inference. While direct application of this method to time series modeling is not straightforward, we represent it in our experiments by sticking to our generic non-linear BNSDE design in (2), and inferring it by maximizing the ELBO:  $\mathcal{L}(\psi, \phi_f, \phi_G) = \mathbb{E}_{\mathbf{Z}, \mathbf{H}, \theta_f, \theta_G} [\log p(\mathbf{Y}|\mathbf{Z})] - D_{KL}(q_{\phi_f}(\theta_f), q_{\phi_G}(\theta_G) || p(\theta_f), p(\theta_G))$ , applying the local reparameterization trick on  $\theta_f$  and  $\theta_G$ . Although variational inference can be seen from a PAC-perspective by choosing the log-likelihood as loss-term ([Knoblauch et al., 2019](#)), the ELBO does not account for the deviation of variational posterior over latent dynamics from the prior latent dynamics. We refer to this baseline in the experiments as *Variational Bayes*. The approximate posterior design here closely follows the PR-SSM approach ([Doerr et al., 2018](#)), which represents the state of the art in state-space modeling.

**Empirical Bayes as PAC Learning.** The learning algorithm of [Look and Kandemir \(2019\)](#) shares our BNSDE modeling assumptions, however, it uses Stochastic Gradient Langevin Dynamics (SGLD) to infer  $\theta_f$  and  $\theta_G$ . This algorithm is equivalent to performing MAP estimation of the model parameters based on model specified in (2) while distorting the gradient updates with decaying Gaussian noise that also determines the learning rate.

**Empirical Bayes as PAC Learning.** There are various approaches to identify a dynamical system that differ in the model class used for fitting the right-hand side of the differential equation. They may also allow for transitional noise (e.g., ([Brunton et al., 2016](#); [Durstewitz, 2016](#))). These approaches could be incorporated into ours, by using their transition likelihood and prior over parameters. As we are mainly interested in how to incorporate prior knowledge into these kinds of models, we chose one such competitor ([Hegde et al., 2019](#)), which allows for the most flexible right-hand side with reported results on the CMU Motion capture dataset (see Table 2).

## 6 Experiments

We evaluate our method on simulated dynamical environments where we can tune the relevance of prior knowledge to ground truth as well as on a real-world time series prediction data set. On the quantitative experiments, we evaluate the below four variants of our method:

- (i) *E-Bayes*. This baseline amounts to plain empirical Bayes without prior knowledge, i.e. training objective in (5) with  $p(\mathbf{h}_{0 \rightarrow T} | \theta_f, \theta_G)$  as a solution to  $d\mathbf{h}_t = f_{\theta_f}(\mathbf{h}_t, t)dt + G_{\theta_G}(\mathbf{h}_t, t)d\beta_t$ . We interpret this variant as applying [Germain et al. \(2016\)](#)’s approach to our BNSDE setup.
- (ii) *E-PAC-Bayes*. Empirical PAC Bayes on the BNSDE using the loss in (13) with an uninformative prior drift, i.e.  $r_\xi(\mathbf{h}_t, t) = 0$ .
- (iii) *E-Bayes-Hybrid*. Same training objective as (i), however with  $Q_{0 \rightarrow T}$  as proposed in (8).
- (iv) *E-PAC-Bayes-Hybrid*. The hybrid model (8) with the same loss as *E-PAC-Bayes*.

For a discussion of the computational cost of each of these methods please as well as further experiments and details on them refer to the appendix.

**Lorenz Attractor.** We study the Lorenz attractor. It has the inherently unsolvable dynamics

$$\begin{aligned} dx_t &= \zeta(y_t - x_t)dt + d\beta_t, \\ dy_t &= (x_t(\kappa - z_t) - y_t)dt + d\beta_t, \\ dz_t &= (x_t y_t - \rho z_t)dt + d\beta_t, \end{aligned}$$

where  $\zeta = 10$ ,  $\kappa = 28$ ,  $\rho = 2.67$ , and  $\beta_t$  is a random variable following Brownian motion with unit diffusion. We generate 2000 observations from the above dynamics initiating the system at

Table 1: An ablation study on the Lorenz attractor to evaluate the contributions of the components to prediction performance in test root mean squared error with standard error over ten repetitions.

Prior knowledge	E-Bayes (Germain et al., 2016)	E-PAC-Bayes (Ours)	E-Bayes-Hybrid (Ours)	E-PAC-Bayes-Hybrid (Ours)
None	$5.65 \pm 0.62$	$6.45 \pm 0.29$	N/A	N/A
$\kappa = \rho = 0, \quad \zeta \sim \mathcal{N}(10, 4)$	N/A	N/A	$3.72 \pm 0.12$	<b><math>3.64 \pm 0.14</math></b>
$\zeta = \rho = 0, \quad \kappa \sim \mathcal{N}(2.67, 4)$	N/A	N/A	$0.87 \pm 0.16$	<b><math>0.83 \pm 0.23</math></b>
$\zeta = \kappa = 0, \quad \rho \sim \mathcal{N}(28, 4)$	N/A	N/A	$1.23 \pm 0.37$	<b><math>1.17 \pm 0.36</math></b>

Table 2: Benchmarking of our method on the CMU Motion Capture Data Set. Performance on 300 future frames for mean predictions is averaged over ten repetitions ( $\pm$  standard deviation).

Model	Reference	Bayesian	Hybrid	+KL	Test MSE $\pm$ Std
DTSBN-S	(Gan et al., 2015)	No	No	No	$34.86 \pm 0.02$
npODE	(Heinonen et al., 2018)	No	No	No	22.96
Neural-ODE	(Chen et al., 2018)	No	No	No	$22.49 \pm 0.88$
ODE <sup>2</sup> VAE	(Yildiz et al., 2019)	Yes	Yes	Yes	$10.06 \pm 1.40$
ODE <sup>2</sup> VAE-KL	(Yildiz et al., 2019)	Yes	Yes	Yes	$8.09 \pm 1.95$
D-BNN (SGLD)	(Look and Kandemir, 2019)	Yes	No	No	$13.89 \pm 2.56$
Variational Bayes	(Hegde et al., 2019)	Yes	No	Yes	$9.55 \pm 2.15$
E-Bayes	(Germain et al., 2016)	Yes	No	No	$10.69 \pm 2.06$
E-PAC-Bayes	Our Contribution	Yes	No	Yes	$8.08 \pm 1.64$
E-Bayes-Hybrid	Our Contribution	Yes	Yes	No	$8.89 \pm 1.87$
E-PAC-Bayes-Hybrid	Our Contribution	Yes	Yes	Yes	<b><math>7.82 \pm 2.18</math></b>

$x_0, y_0, z_0 = (1, 1, 28)$ , use the first half for training and the rest for test. We split the training data into 20 sequences of length 50, which can be seen as i.i.d. samples of the system with different initial states. Table 1 presents the 100-step ahead forecasting error in MSE on the test set for our model variants, where the models always have prior knowledge on one parameter, assuming the other two to be zero. Despite the imprecision of the provided prior knowledge, the largest performance leap comes from the hybrid models. While the complexity term on the PAC bound only restricts the model capacity for black-box system identification, it brings consistent benefit on the hybrid setup. Figure 1 visualizes the predicted trajectories on the test sequence for prior knowledge on  $dz_t$  as detailed in Table 1 mapped of the  $x$ -coordinate over time. Even with weak prior knowledge, the proposed model is stable a lot longer than the baseline as well as showing a proper increase in the variance as the predicted trajectory increases, while the baseline diverges a lot sooner without a proper increase in uncertainty. See the appendix for a more detailed discussion and further figures.

**CMU Walking Data Set.** We benchmark our method against the state of the art on the CMU Walking data set sticking to the setup in Yildiz et al. (2019). We train an *E-PAC-Bayes* model on the MOCAP-1 data set that consists of 43 motion capture sequences measured from 43 different subjects.

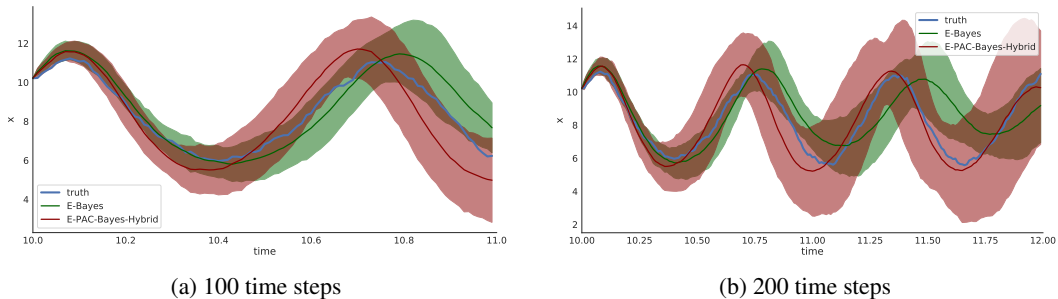


Figure 1: Predicted trajectory of the Lorenz data set mapped to one dimension with and without prior knowledge. The error bars indicate  $\pm 2$  standard deviations over 21 trajectories.



The drift net of the learned BNSDE is then treated as vague prior knowledge on human walking dynamics. We use MOCAP-2 with 23 walking sequences from Subject 35 to represent a high-fidelity subject-specific modeling task. As common, we report the test MSE of our method, its close variants, and several of state-of-the-art methods in Table 2. The method obtains the best performance when all components of our objective are active. Unlike the Lorenz experiment, our method achieves competitive prediction accuracy even when the PAC prior is provided only for regularization purposes and without prior knowledge, as expected due to the importance of stability in SDE training.

## 7 Extensions and Limitations

Our method is versatile and easily adaptable to other solvers than the Euler-Maruyama discretization scheme. The training loss derived in (5) can also be optimized using a closed-form Gaussian assumed density scheme applied over a stochastic Runge-Kutta variant (Li et al., 2019). The proposed Empirical PAC Bayes algorithm can generalize beyond the SDE context to any feed-forward or prediction task with little effort. Our tied gradient update procedure allows training on the loose bound while providing generalization guarantees on its tighter counterpart. Our stochastic approximation of the data-loglikelihood currently relies on samples obtained from the prior, yet could be improved by e.g. incorporating an importance sampling scheme using particle filtering (Kantas et al., 2015). As the PAC bound provided in (5) has the potential to be vacuous for most choices of drift and diffusion nets, incorporating a Hoeffding assumption (Alquier et al., 2016) can further tighten it.

### Broader Impact

The proposed approach allows for a principled way of incorporating prior knowledge into the learning stochastic differential equations, together with the flexibility and strength of deep Bayesian neural nets. As such it shares the potential benefits and risks of both. The growing field of combining differential equations with neural networks has great potential as it allows for a combination of the often disjoint strands of mostly data-driven approaches (deep learning) with mostly symbolic, i.e. model-driven, approaches (differential equations), combining the best of both worlds by offering both the possibility of improved predictive performance as well as greater interpretability. SDEs are agnostic to the task at hand and so the proposed method inherits both their beneficial potential as a powerful tool in many fields of science as well as their ethically doubtful applications.

It also inherits from deep learning the downsides of potential susceptibility to problems such as adversarial attacks and predictive overconfidence. There is growing literature indicating that the Bayesian approach to neural nets we use seem to be more robust against such problems than standard deterministic nets, but most of that is ongoing research without final results. Note that we are not aware of any work showing adversarial attacks in the neural network + differential equation literature but this should of course not be read as a proof of absence. Summarizing the broader impact in one sentence, our proposed approach as well as other work in this direction has the potential of reinforcing the positive as well as negative influence differential equations are already having, without being able to offer guarantee only benefits. The ethical responsibility remains with the scientist/engineer building on top of it.

### References

- P. Alquier, J. Ridgway, and N. Chopin. On the properties of variational approximations of gibbs posteriors. *The Journal of Machine Learning Research*, 17(1):8374–8414, 2016.
- C. Archambeau, M. Opper, Y. Shen, D. Cornford, and J.S. Shawe-Taylor. Variational Inference for Diffusion Processes. In *NIPS*. 2008.
- S. L Brunton, J.L. Proctor, and J.N. Kutz. Discovering governing equations from data by sparse identification of nonlinear dynamical systems. *Proceedings of the national academy of sciences*, 113(15):3932–3937, 2016.
- O. Catoni. PAC-Bayesian Supervised Classification: The Thermodynamics of Statistical Learning. *IMS Lecture Notes Monograph Series*, 56, 2007.

- R. Chen, Y. Rubanova, J. Bettencourt, and D. Duvenaud. Neural Ordinary Differential Equations. In *NeurIPS*, 2018.
- A.G. de G. Matthews, J. Hensman, R.E. Turner, and Z. Ghahramani. On Sparse Variational Methods and the Kullback-Leibler Divergence between Stochastic Processes. *AISTATS*, 2016.
- A. Doerr, C. Daniel, M. Schiegg, D. Nguyen-Tuong, S. Schaal, M. Toussaint, and S. Trimpe. Probabilistic Recurrent State-Space Models. In *ICML*, 2018.
- D. Durstewitz. A state space approach for piecewise-linear recurrent neural networks for reconstructing nonlinear dynamics from neural measurements. *arXiv preprint arXiv:1612.07846*, 2016.
- G. Dziugaite and D.M. Roy. Computing Nonvacuous Generalization Bounds for Deep (Stochastic) Neural Networks with Many More Parameters than Training Data. In *UAI*, 2017.
- B. Efron. *Large-scale Inference: Empirical Bayes Methods for Estimation, Testing, and Prediction*, volume 1. Cambridge University Press, 2012.
- Z. Gan, C. Li, R. Henao, D.E. Carlson, and L. Carin. Deep Temporal Sigmoid Belief Networks for Sequence Modeling. In *NIPS*, 2015.
- M. Garnelo, D. Rosenbaum, C. Maddison, T. Ramalho, D. Saxton, M. Shanahan, Y.W. Teh, D. Rezende, and S. M.A. Eslami. Conditional Neural Processes. *ICML*, 2018.
- P. Germain, F. Bach, A. Lacoste, and S. Lacoste-Julien. PAC-Bayesian Theory Meets Bayesian Inference. In *NIPS*, 2016.
- P. Hegde, M. Heinonen, H. Lähdesmäki, and S. Kaski. Deep Learning with Differential Gaussian Process Flows. In *AISTATS*, 2019.
- M. Heinonen, C. Yildiz, H. Mannerström, J. Intosalmi, and H. Lähdesmäki. Learning Unknown ODE Models with Gaussian Processes. In *ICML*, 2018.
- N. Kantas, A. Doucet, S.S. Singh, J. Maciejowski, N. Chopin, et al. On particle methods for parameter estimation in state-space models. *Statistical science*, 30(3):328–351, 2015.
- R.E. Kass and A.E. Raftery. Bayes Factors. *Journal of the American Statistical Association*, 90(430): 773–795, 1995.
- D.P. Kingma, T. Salimans, and M. Welling. Variational Dropout and The Local Reparameterization Trick. In *NIPS*, 2015.
- P.E. Kloeden and E. Platen. *Numerical Solution of Stochastic Differential Equations*. Springer-Verlag, 2011.
- J. Knoblauch, J. Jewson, and T. Damoulas. Generalized variational inference. *arXiv preprint arXiv:1904.02063*, 2019.
- X. Li, Y. Wu, L. Mackey, and M.A. Erdogdu. Stochastic Runge-Kutta accelerates Langevin Monte Carlo and beyond. In *NeurIPS*. 2019.
- A. Look and M. Kandemir. Differential Bayesian Neural Nets. In *4th NeurIPS Workshop on Bayesian Deep Learning*, 2019.
- A. Malinin and M. Gales. Predictive uncertainty estimation via prior networks. In *NeurIPS*, 2018.
- A. Maurer. A note on the PAC Bayesian theorem. *arXiv preprint cs/0411099*, 2004.
- D. McAllester. PAC-Bayesian Model Averaging. In *COLT*, 1999.
- B. Oksendal. *Stochastic Differential Equations: An Introduction with Applications*. Springer-Verlag, 1992.
- D. Reeb, A. Doerr, S. Gerwinn, and B. Rakitsch. Learning Gaussian Processes by Minimizing PAC-Bayesian Generalization Bounds. In *NeurIPS*, 2018.

- M. Seeger. PAC-Bayesian Generalisation Error Bounds for Gaussian Process Classification. *Journal of Machine Learning Research*, 3:233–269, 2002.
- M. Sensoy, L. Kaplan, and M. Kandemir. Evidential Deep Learning to Quantify Classification Uncertainty. In *NeurIPS*, 2018.
- C. Yildiz, M. Heinonen, and H. Lahdesmaki. ODE2VAE: Deep Generative Second Order ODEs with Bayesian Neural Networks. In *NeurIPS*. 2019.

# APPENDIX

## A Continuous time SDEs

Solving the SDE system in (2) for a time interval  $[0, T]$  and fixed  $\theta_f, \theta_G$  requires computing integrals of the form

$$\int_0^T d\mathbf{h}_t = \int_0^T f_{\theta_f}(\mathbf{h}_t, t) dt + \int_0^T G_{\theta_G}(\mathbf{h}_t, t) d\beta_t.$$

This operation is intractable for almost any practical choice of  $f_{\theta_f}(\cdot, \cdot)$  and  $G_{\theta_G}(\cdot, \cdot)$  for two reasons. First, the integral around the drift term  $f_{\theta_f}(\cdot, \cdot)$  does not have an analytical solution, due both to potential nonlinearities of the drift and to the fact that  $\mathbf{h}_t \sim p(\mathbf{h}_t, t)$  is a stochastic variable following an implicitly defined distribution. Second, the diffusion term involves the Itô integral (Oksendal, 1992) about  $\beta_t$  which multiplies the non-linear function  $G_{\theta_G}(\cdot, \cdot)$ .

For each of the SDEs in (8) and (9), we could alternatively to the Euler-Maruyama integration theme use the Fokker-Planck-Kolmogorov equation to derive a partial differential equation (PDE) system

$$\begin{aligned} \partial p_{\text{hyb}}(\mathbf{h}_t, t | \theta_f, \theta_G) / \partial t &= -\nabla \cdot [(f_{\theta_f}(\mathbf{h}_t, t) + \gamma \circ r_\xi(\mathbf{h}_t, t)) p_{\text{hyb}}(\mathbf{h}_t, t | \theta_f, \theta_G)] \\ &\quad + \nabla \cdot (e \nabla \cdot G_{\theta_G}(\mathbf{h}_t, t) p_{\text{hyb}}(\mathbf{h}_t, t | \theta_f, \theta_G)), \\ \partial p_{\text{pri}}(\mathbf{h}_t, t | \theta_G) / \partial t &= -\nabla \cdot [\gamma \circ r_\xi(\mathbf{h}_t, t) p_{\text{pri}}(\mathbf{h}_t, t | \theta_G)] \\ &\quad + \nabla \cdot (e \nabla \cdot G_{\theta_G}(\mathbf{h}_t, t) p_{\text{pri}}(\mathbf{h}_t, t | \theta_G)), \end{aligned}$$

where  $\nabla \cdot$  is the divergence operator and  $e = (1, \dots, 1)^\top$ . Theoretically, these distributions can be obtained by solving the Fokker-Planck PDE. As this requires solving a PDE which is not analytically tractable, we instead resort to the discrete time Euler-Maruyama integration.

## B Proofs

This section gives a more detailed derivation of the individual results stated in the main paper.

**Lemma 1.** *For two process distributions  $Q_{0 \rightarrow T}$  and  $P_{0 \rightarrow T}$  defined as in the main paper, the following property holds*

$$\begin{aligned} D_{KL}(Q_{0 \rightarrow T} || P_{0 \rightarrow T}) &= \frac{1}{2} \int_0^T \mathbb{E}_{Q_{0 \rightarrow T}} [f_{\theta_f}(\mathbf{h}_t, t)^T \mathbf{J}_t^{-1} f_{\theta_f}(\mathbf{h}_t, t)] dt \\ &\quad + D_{KL}(q(\theta_f) || p(\theta_f)) + D_{KL}(q(\theta_G) || p(\theta_G)) \end{aligned}$$

for some  $T > 0$ , where  $\mathbf{J}_t = G_{\theta_G}(\mathbf{h}_t, t) G_{\theta_G}(\mathbf{h}_t, t)^T$ .

**Proof.** Assume Euler-Maruyama discretization for the process  $Q_{0 \rightarrow T}$  on arbitrarily chosen  $K$  time points within the interval  $[0, T]$ . Then we have  $D_{KL}(Q || P)$  denoting the Kullback-Leibler divergence between processes  $Q_{0 \rightarrow T}$  and  $P_{0 \rightarrow T}$  up to discretization into  $T$  time points as:

$$\begin{aligned} D_{KL}(Q || P) &= \iiint \log \frac{\prod_{t=0}^{K-1} (p_{\psi}(\mathbf{z}_t | \mathbf{h}_t) \mathcal{N}(\mathbf{h}_{t+1} | (f_{\theta_f}(\mathbf{h}_t, t) + \gamma \circ r_\xi(\mathbf{h}_t, t)) \Delta t, \mathbf{J}_t \Delta t))}{\prod_{t=0}^{K-1} (p_{\psi}(\mathbf{z}_t | \mathbf{h}_t) \mathcal{N}(\mathbf{h}_{t+1} | \gamma \circ r_\xi(\mathbf{h}_t, t) \Delta t, \mathbf{J}_t \Delta t))} \\ &\quad \frac{p(\mathbf{h}_0) q(\theta_f) q(\theta_G)}{p(\mathbf{h}_0) p(\theta_f) p(\theta_G)} Q_{0 \rightarrow T} d\mathbf{Z} d\mathbf{H} d\theta_f d\theta_G \\ &= \sum_{t=0}^{K-1} \iiint \log \mathcal{N}(\mathbf{h}_{t+1} | (f_{\theta_f}(\mathbf{h}_t, t) + \gamma \circ r_\xi(\mathbf{h}_t, t)) \Delta t, \mathbf{J}_t \Delta t) \\ &\quad - \log \mathcal{N}(\mathbf{h}_{t+1} | \gamma \circ r_\xi(\mathbf{h}_t, t) \Delta t, \mathbf{J}_t \Delta t) Q_{0 \rightarrow T} d\mathbf{H} d\theta_f d\theta_G \\ &\quad + D_{KL}(q(\theta_f) || p(\theta_f)) + D_{KL}(q(\theta_G) || p(\theta_G)). \end{aligned}$$

Above in the second line we drop the integral around  $p_\psi(\mathbf{z}_t|\mathbf{h}_t)$  as no term is left that depends on  $\mathbf{z}_t$ , hence the distribution integrates out to unity. For simplicity, let us modify notation and adopt:  $\mathbf{f}_t := f_{\theta_f}(\mathbf{h}_t, t) - \gamma \circ r_\xi(\mathbf{h}_t, t)$ ,  $\mathbf{g}_t := -\gamma \circ r_\xi(\mathbf{h}_t, t)$ , and  $\Delta\mathbf{h}_{t+1} := \mathbf{h}_{t+1} - \mathbf{h}_t$ . Now writing down the  $\log(\cdot)$  terms explicitly, we get

$$\begin{aligned} D_{KL}(Q||P) &= \frac{1}{2} \sum_{t=0}^{K-1} \iiint \left[ -(\Delta\mathbf{h}_{t+1} - \mathbf{f}_t\Delta t)^T (\mathbf{J}_t\Delta t)^{-1} (\Delta\mathbf{h}_{t+1} - \mathbf{f}_t\Delta t) \right. \\ &\quad \left. + (\Delta\mathbf{h}_{t+1} - \mathbf{g}_t\Delta t)^T (\mathbf{J}_t\Delta t)^{-1} (\Delta\mathbf{h}_{t+1} - \mathbf{g}_t\Delta t) \right] \\ &\quad \cdot p_{\text{hyb}}(\mathbf{h}_{0 \rightarrow T}|\theta_f, \theta_G) q_{\phi_f}(\theta_f) q_{\phi_G}(\theta_G) d\mathbf{H} d\theta_f d\theta_G \\ &\quad + D_{KL}(q(\theta_f)||p(\theta_f)) + D_{KL}(q(\theta_G)||p(\theta_G)). \end{aligned}$$

Expanding the products, removing the canceling out terms, and rearranging the rest, we get

$$\begin{aligned} D_{KL}(Q||P) &= \frac{1}{2} \sum_{t=0}^{K-1} \iiint \left[ -\mathbf{f}_t^T \mathbf{J}_t^{-1} \mathbf{f}_t \Delta t + 2\Delta\mathbf{h}_{t+1} \mathbf{J}_t^{-1} \mathbf{f}_t + \mathbf{g}_t^T \mathbf{J}_t^{-1} \mathbf{g}_t \Delta t - 2\Delta\mathbf{h}_{t+1} \mathbf{J}_t^{-1} \mathbf{g}_t \right] \\ &\quad \cdot p_{\text{hyb}}(\mathbf{h}_{0 \rightarrow T}|\theta_f, \theta_G) q_{\phi_f}(\theta_f) q_{\phi_G}(\theta_G) d\mathbf{H} d\theta_f d\theta_G \\ &\quad + D_{KL}(q(\theta_f)||p(\theta_f)) + D_{KL}(q(\theta_G)||p(\theta_G)). \end{aligned}$$

Note that from the definition of the process it follows that

$$\int \Delta\mathbf{h}_{t+1} p_{\text{hyb}}(\mathbf{h}_{0 \rightarrow T}|\theta_f, \theta_G) d\Delta\mathbf{h}_{t+1} = \mathbf{f}_t \Delta t.$$

Plugging this fact into the KL term, we have

$$\begin{aligned} D_{KL}(Q||P) &= \frac{1}{2} \sum_{t=0}^{K-1} \iiint \left[ \mathbf{f}_t^T \mathbf{J}_t^{-1} \mathbf{f}_t \Delta t + \mathbf{g}_t^T \mathbf{J}_t^{-1} \mathbf{g}_t \Delta t - 2\mathbf{f}_t \mathbf{J}_t^{-1} \mathbf{g}_t \Delta t \right] q_{\phi_f}(\theta_f) q_{\phi_G}(\theta_G) d\theta_f d\theta_G \\ &\quad + D_{KL}(q(\theta_f)||p(\theta_f)) + D_{KL}(q(\theta_G)||p(\theta_G)). \end{aligned}$$

For any pair of vectors  $\mathbf{a}, \mathbf{b} \in \mathbb{R}^P$  and symmetric matrix  $\mathbf{C} \in \mathbb{R}^{P \times P}$ , the following identity holds:

$$\mathbf{a}^T \mathbf{C} \mathbf{a} - \mathbf{b}^T \mathbf{C} \mathbf{b} = (\mathbf{a} - \mathbf{b})^T \mathbf{C} (\mathbf{a} - \mathbf{b}) + 2\mathbf{a}^T \mathbf{C} \mathbf{b}.$$

Applying this identity to the above, we attain

$$\begin{aligned} D_{KL}(Q||P) &= \frac{1}{2} \sum_{t=0}^{K-1} \iiint \left[ (\mathbf{f}_t - \mathbf{g}_t)^T \mathbf{J}_t^{-1} (\mathbf{f}_t - \mathbf{g}_t) \Delta t \right] q_{\phi_f}(\theta_f) q_{\phi_G}(\theta_G) d\theta_f d\theta_G \\ &\quad + D_{KL}(q(\theta_f)||p(\theta_f)) + D_{KL}(q(\theta_G)||p(\theta_G)). \end{aligned}$$

Plugging back the original terms and setting  $K$  to the limit, we arrive at the desired outcome

$$\begin{aligned} &\lim_{K \rightarrow +\infty} \left\{ \frac{1}{2} \sum_{t=0}^{K-1} \iiint \left[ (f_{\theta_f}(\mathbf{h}_t, t))^T \mathbf{J}_t^{-1} f_{\theta_f}(\mathbf{h}_t, t) \Delta t \right] q_{\phi_f}(\theta_f) q_{\phi_G}(\theta_G) d\theta_f d\theta_G \right. \\ &\quad \left. + D_{KL}(q(\theta_f)||p(\theta_f)) + D_{KL}(q(\theta_G)||p(\theta_G)) \right\} \\ &= \frac{1}{2} \int \left[ \iint f_{\theta_f}(\mathbf{h}_t, t)^T \mathbf{J}_t^{-1} f_{\theta_f}(\mathbf{h}_t, t) q_{\phi_f}(\theta_f) q_{\phi_G}(\theta_G) d\theta_f d\theta_G \right] dt \\ &\quad + D_{KL}(q(\theta_f)||p(\theta_f)) + D_{KL}(q(\theta_G)||p(\theta_G)) \\ &= \frac{1}{2} \int_0^T \mathbb{E}_{Q_{0 \rightarrow T}} \left[ f_{\theta_f}(\mathbf{h}_t, t)^T \mathbf{J}_t^{-1} f_{\theta_f}(\mathbf{h}_t, t) \right] dt + D_{KL}(q(\theta_f)||p(\theta_f)) \\ &\quad + D_{KL}(q(\theta_G)||p(\theta_G)). \end{aligned}$$

□

**Theorem 1.** Let  $p(\mathbf{y}_t|\mathbf{z}_t)$  be uniformly bounded likelihood function with density  $p(\mathbf{y}_t|\mathbf{z}_t)$  everywhere,  $p_\psi(\mathbf{z}_t|\mathbf{h}_t)$  be an also bounded observation model, and  $Q_{0 \rightarrow T}$  and  $P_{0 \rightarrow T}$  be the joints of the posterior and prior stochastic processes defined on the hypothesis class of the learning task, respectively. Define the true risk of a draw from  $Q_{0 \rightarrow T}$  on an i.i.d. sample  $\mathbf{Y} = \{\mathbf{y}_1, \dots, \mathbf{y}_K\}$  at discrete and potentially irregular time points  $t_1, \dots, t_K$  drawn from an unknown ground-truth stochastic process  $G(t)$  as the expected model misfit as on the sample as defined via the following risk over hypotheses  $Q = \mathbf{z}_{0 \rightarrow T}, \mathbf{h}_{0 \rightarrow T}, \theta_f, \theta_G$  for an arbitrary, but bounded choice of  $q(\theta_G)q(\theta_f)$

$$R(Q) = -\mathbb{E}_{\mathbf{Y} \sim G(t)} \left[ \prod_{k=1}^K \left[ p(\mathbf{y}_k|\mathbf{z}_k)p(\mathbf{z}_k|\mathbf{h}_k)q(\mathbf{h}_k|\mathbf{h}_{k-1}, \theta_f, \theta_G) \right] p(\mathbf{h}_0)q(\theta_f)q(\theta_G) \right], \quad (14)$$

for time horizon  $T > 0$  and the corresponding empirical risk on a data set  $\mathcal{D} = \{\mathbf{Y}_1, \dots, \mathbf{Y}_N\}$  as

$$R_{\mathcal{D}}(Q) = -\frac{1}{N} \sum_{n=1}^N \left[ \prod_{k=1}^K \left[ p(\mathbf{y}_k^n|\mathbf{z}_k^n)p(\mathbf{z}_k^n|\mathbf{h}_k^n)q(\mathbf{h}_k^n|\mathbf{h}_{k-1}^n, \theta_f, \theta_G) \right] p(\mathbf{h}_0^n)q(\theta_f)q(\theta_G) \right]. \quad (15)$$

Then the expected true risk is bounded above by the marginal negative log-likelihood of the predictor and a complexity functional as

$$\begin{aligned} \mathbb{E}_{Q_{0 \rightarrow T}} [R(Q)] &\leq \mathbb{E}_{Q_{0 \rightarrow T}} [R_{\mathcal{D}}(Q)] + \mathcal{C}_\delta(Q_{0 \rightarrow T}, P_{0 \rightarrow T}), \quad (16) \\ &\leq -\frac{1}{SN} \sum_{n=1}^N \sum_{s=1}^S \left\{ \left[ \sum_{k=1}^K \ln \left( p(\mathbf{y}_k^n|\mathbf{z}_k^{s,n})p(\mathbf{z}_k^{s,n}|\mathbf{h}_k^{s,n}) q(\mathbf{h}_k^{s,n}|\mathbf{h}_{k-1}^{s,n}, \theta_f^{s,n}, \theta_G^{s,n})p(\mathbf{h}_0^{s,n}) \right) \right] \right. \\ &\quad \left. + \ln q(\theta_f^{s,n}) + \ln q(\theta_G^{s,n}) \right\} + \mathcal{C}_{\delta/2}(Q_{0 \rightarrow T}, P_{0 \rightarrow T}) + \sqrt{\frac{\ln(2N/\delta)}{2S}} + K \ln \bar{B}, \quad (17) \end{aligned}$$

where  $\bar{B} := \max_{\mathbf{y}_k, \mathbf{h}_k, \theta_f, \theta_G} p(\mathbf{y}_k, \mathbf{h}_k|\theta_f, \theta_G)q(\theta_f)q(\theta_G)$  is the uniform bound,  $S$  is the sample count taken independently for each observed sequence, and the complexity functional is given as

$$\mathcal{C}_\delta(Q_{0 \rightarrow T}, P_{0 \rightarrow T}) := \sqrt{1/(2N)} \sqrt{D_{KL}(Q_{0 \rightarrow T}||P_{0 \rightarrow T}) + \ln(2\sqrt{N}) - \ln(\delta/2)}$$

with  $D_{KL}(Q_{0 \rightarrow T}||P_{0 \rightarrow T})$  as in Lemma 1 for some  $\delta > 0$ .

**Proof.** To be able to apply known PAC bounds, we first define the hypothesis class  $\mathfrak{h} \in \mathcal{H}_K$  that contain latent states  $\mathbf{z}_k, \mathbf{h}_k, \theta_f, \theta_G$  that explain the observations  $\mathbf{y}_k$ . Then, we define the true risk as

$$R(\mathfrak{h}) = \mathbb{E}_{\mathbf{Y}_k \sim G(t)} \left[ 1 - \frac{1}{\bar{B}_K} \underbrace{\left( \prod_{k=1}^K p(\mathbf{y}_k|\mathbf{z}_k)p(\mathbf{z}_k|\mathbf{h}_k)q(\mathbf{h}_k|\mathbf{h}_{k-1}, \theta_f, \theta_G) \right)}_{=: p(\mathbf{y}_k; Q)} p(\mathbf{h}_0)q(\theta_f)q(\theta_G) \right]$$

and the empirical risk as

$$R_{\mathcal{D}}(\mathfrak{h}) = \frac{1}{N} \sum_{n=1}^N \left\{ 1 - \frac{1}{\bar{B}_K} \left( \prod_{kn=1}^K p(\mathbf{y}_k^n|\mathbf{z}_k^n)p(\mathbf{z}_k^n|\mathbf{h}_k^n)q(\mathbf{h}_k^n|\mathbf{h}_{k-1}^n, \theta_f^n, \theta_G^n) \right) p(\mathbf{h}_0^n)q(\theta_f^n)q(\theta_G^n) \right\},$$

where we defined

$$\bar{B}_K := \max_{\mathbf{y}, \mathbf{z}_k, \mathbf{h}_k, \theta_f, \theta_G} \prod_{k=1}^K p(\mathbf{y}, \mathbf{z}_k, \mathbf{h}_k, \theta_f, \theta_G) \leq \left( \max_{\mathbf{y}, \mathbf{z}_k, \mathbf{h}_k, \theta_f, \theta_G} p(\mathbf{y}, \mathbf{z}_k, \mathbf{h}_k, \theta_f, \theta_G) \right)^K.$$

The data set  $\mathcal{D} = \{\mathbf{Y}_k^n\}_{k,n}$  was generated by an unknown stochastic process  $G(t)$ . Note that we normalize the risks  $R(\mathfrak{h})$  and  $R_{\mathcal{D}}(\mathfrak{h})$  by the maximum of the likelihood and thereby obtaining a possible range of these risk of  $[0, 1]$ . The likelihood can be bounded, as each term  $p(\mathbf{y}_k|\mathbf{z}_k), p(\mathbf{z}_k|\mathbf{h}_k), q(\mathbf{h}_k|\mathbf{h}_{k-1}, \theta_f, \theta_G), q(\theta_f), q(\theta_G)$  can be bounded from above:

$p(\mathbf{y}_k|\mathbf{z}_k)$  We model this by a Gaussian, therefore, it is bounded, if we assume a minimal allowed variance.



$p(\mathbf{z}_k | \mathbf{h}_k)$  This is also modeled with a Gaussian with a minimal allowed variance, hence is bounded by above by the inverse of the minimal standard deviation.

$q(\mathbf{h}_k | \mathbf{h}_{k-1}, \theta_f, \theta_G)$  This term corresponds to an Euler-Maruyama step. Therefore, it can again be bounded allowing for a minimal variance.

$q(\theta_f), q(\theta_G)$  These two terms are model choices and therefore can directly be designed to be bounded by above (for example, again using a Gaussian distribution with a bound on the minimal variance).

To obtain a tractable bound, it is common practice is to upper bound its analytically intractable inverse (Germain et al., 2016) using Pinsker's inequality (Catoni, 2007; Dziugaite and Roy, 2017). Here, we rely on the following theorem

**PAC-theorem (Maurer, 2004)** For any  $[0, 1]$ -valued loss function giving rise to empirical and true risk  $R_{\mathcal{D}}(\mathbf{h}), R(\mathbf{h})$ , for any distribution  $\Delta$ , for any  $N \in \mathbb{N}$ , for any distribution  $P_{0 \rightarrow T}$  on a hypothesis set  $\mathcal{Q}_K$ , and for any  $\delta \in (0, 1]$ , the following holds with probability at least  $1 - \delta$  over the training set  $\mathcal{D} \sim \Delta^N$ :

$$\forall Q_{0 \rightarrow T} : \mathbb{E}_{\mathbf{h} \sim Q_{0 \rightarrow T}} [R(\mathbf{h})] \leq \mathbb{E}_{\mathbf{h} \sim Q_{0 \rightarrow T}} [R_{\mathcal{D}}(\mathbf{h})] + \sqrt{\frac{\text{KL}(Q_{0 \rightarrow T} \parallel P_{0 \rightarrow T}) + \ln\left(\frac{2\sqrt{N}}{\delta}\right)}{2N}}$$

Here,  $\text{KL}(Q_{0 \rightarrow T} \parallel P_{0 \rightarrow T})$  acts as a complexity measure that measures, how much the posterior predictive governing SDE  $Q_{0 \rightarrow T}$  needed to be adapted to the data when compared to an a priori chosen SDE that could alternatively have generated data  $P_{0 \rightarrow T}$ . In our situation,  $Q_{0 \rightarrow T}$  is obtained by our approximation scheme, resulting in a bounded likelihood of observations  $\mathbf{y}_k$  which factorizes over different observations  $n$ . As  $P_{0 \rightarrow T}$  can be arbitrarily chosen as long as it does not depend on the observations. As mentioned in the main paper, we chose an SDE with the same diffusion term which also factorizes over observations. Using this setting, we can analytically compute the KL-distance, see Lemma 1.

In order to use the right hand side of this PAC-bound, we need to evaluate  $\mathbb{E}_{\mathbf{h} \sim Q_{0 \rightarrow T}} [R_{\mathcal{D}}(\mathbf{h})]$ . To this end, we note the following:

$$\begin{aligned} & \mathbb{E}_{\mathbf{h} \sim Q_{0 \rightarrow T}} [R_{\mathcal{D}}(\mathbf{h})] \\ &= \frac{1}{N} \sum_{n=1}^N \mathbb{E}_{\mathbf{h} \sim Q_{0 \rightarrow T}} \left[ 1 - \frac{1}{\bar{B}_K} \left( \prod_{k=1}^K p(\mathbf{y}_k^n | \mathbf{z}_k^n) p(\mathbf{z}_k^n | \mathbf{h}_k^n) q(\mathbf{h}_k^n | \mathbf{h}_{k-1}^n, \theta_f^n, \theta_G^n) \right) p(\mathbf{h}_0^n) q(\theta_f^n) q(\theta_G^n) \right] \\ &= 1 - \frac{1}{N} \sum_{n=1}^N \mathbb{E}_{\mathbf{h} \sim Q_{0 \rightarrow T}} \left[ \left( \frac{1}{\bar{B}_K} \prod_{k=1}^K p(\mathbf{y}_k^n | \mathbf{z}_k^n) p(\mathbf{z}_k^n | \mathbf{h}_k^n) q(\mathbf{h}_k^n | \mathbf{h}_{k-1}^n, \theta_f^n, \theta_G^n) \right) p(\mathbf{h}_0^n) q(\theta_f^n) q(\theta_G^n) \right] \\ &\stackrel{\text{Hoeffding}}{\leq} 1 - \frac{1}{SN} \sum_{n=1}^N \sum_{s=1}^S \left[ \left( \frac{1}{\bar{B}_K} \prod_{k=1}^K p(\mathbf{y}_k^{n,s} | \mathbf{z}_k^{n,s}) p(\mathbf{z}_k^{n,s} | \mathbf{h}_k^{n,s}) q(\mathbf{h}_k^{n,s} | \mathbf{h}_{k-1}^{n,s}, \theta_f^{n,s}, \theta_G^{n,s}) \right) \right. \\ &\quad \left. \cdot p(\mathbf{h}_0^{n,s}) q(\theta_f^{n,s}) q(\theta_G^{n,s}) \right] + \sqrt{\frac{\log(2N/\delta)}{2S}} \\ &\stackrel{-\log(z) \geq 1-z}{\leq} -\frac{1}{SN} \sum_{n=1}^N \sum_{s=1}^S \left[ \log \left( \prod_{k=1}^K p(\mathbf{y}_k^{n,s} | \mathbf{z}_k^{n,s}) p(\mathbf{z}_k^{n,s} | \mathbf{h}_k^{n,s}) q(\mathbf{h}_k^{n,s} | \mathbf{h}_{k-1}^{n,s}, \theta_f^{n,s}, \theta_G^{n,s}) \right) \right. \\ &\quad \left. \cdot p(\mathbf{h}_0^{n,s}) q(\theta_f^{n,s}) q(\theta_G^{n,s}) + \log \bar{B}_K + \sqrt{\frac{\log(2N/\delta)}{2S}} \right] \\ &= -\frac{1}{SN} \sum_{n=1}^N \sum_{s=1}^S \sum_{k=1}^K \left[ \log \left( p(\mathbf{y}_k^{n,s} | \mathbf{z}_k^{n,s}) p(\mathbf{z}_k^{n,s} | \mathbf{h}_k^{n,s}) q(\mathbf{h}_k^{n,s} | \mathbf{h}_{k-1}^{n,s}, \theta_f^{n,s}, \theta_G^{n,s}) \right) \right. \\ &\quad \left. \cdot p(\mathbf{h}_0^{n,s}) q(\theta_f^{n,s}) q(\theta_G^{n,s}) + \log \bar{B}_K + \sqrt{\frac{\log(2N/\delta)}{2S}} \right], \end{aligned}$$

where we have used Hoeffding's inequality for estimating the true marginal likelihood with a  $K$  samples trace  $\mathbf{z}_k^s, \mathbf{h}_k^s, \theta_f^s, \theta_G^s, k = 1, \dots, K, s = 1, \dots, S$  for each observation. As we approximate the true marginal likelihood for each time-series  $n$  separately via sampling, we require Hoeffding to hold simultaneously for all  $n$ . Using a union bound, we have to scale  $\delta$  for each  $n$  by  $N$ . Splitting confidences between the PAC-bound and the sampling based approximation results an additional factor of 2. With  $\delta/(2N)$ , the corresponding inequality holds with a probability of  $P > \delta/2$ . Also using  $\delta/2$  in PAC-theorem, we obtain that with  $P \geq 1 - \delta$  we have for all  $Q_{0 \rightarrow T}$  that

$$\begin{aligned} \mathbb{E}_{\mathbf{h} \sim Q_{0 \rightarrow T}} [R(\mathbf{h})] &\leq \mathbb{E}_{\mathbf{h} \sim Q_{0 \rightarrow T}} [R_{\mathcal{D}}(\mathbf{h})] + \sqrt{\frac{\text{KL}(Q_{0 \rightarrow T} \parallel P_{0 \rightarrow T}) + \ln\left(\frac{2\sqrt{N}}{\delta/2}\right)}{2N}} \\ &\leq -\frac{1}{SN} \sum_{n=1}^N \sum_{s=1}^S \sum_{k=1}^K \left[ \log \left( p(\mathbf{y}_k^n | \mathbf{z}_k^{n,s}) p(\mathbf{z}_k^{n,s} | \mathbf{h}_k^{n,s}) q(\mathbf{h}_k^{n,s} | \mathbf{h}_{k-1}^{n,s}, \theta_f^{n,s}, \theta_G^{n,s}) \right) p(\mathbf{h}_0^{n,s}) q(\theta_f^{n,s}) q(\theta_G^{n,s}) \right] \\ &\quad + \sqrt{\frac{\text{KL}(Q_{0 \rightarrow T} \parallel P_{0 \rightarrow T}) + \ln\left(\frac{2\sqrt{N}}{\delta/2}\right)}{2N}} + \log \bar{B}_K + \sqrt{\frac{\log(2N/\delta)}{2S}} \end{aligned}$$

□

**Lemma 2.** Given a  $L$ -Lipschitz continuous function set

$$\left\{ f_{\theta}^n(x) : \mathbb{R} \rightarrow [0, 1] \mid n = 1, \dots, N \right\} \cup \left\{ g_{\theta}(x) : \mathbb{R} \rightarrow [0, +\infty] \right\},$$

for the two losses:

$$l_1(\theta) = -\sum_{n=1}^N f_{\theta}^n(x) + g_{\theta}(x) \quad \text{and} \quad l_2(\theta) = -\sum_{n=1}^N \ln f_{\theta}^n(x) + g_{\theta}(x),$$

the sequential updates ( $\theta^0 := \theta$ )

$$\begin{aligned} \theta^{(n)} &\leftarrow \theta^{(n-1)} + \alpha_n \nabla (\ln f_{\theta^{(n-1)}}^n(x)), \quad n = 1, \dots, N, \\ \theta^{(N+1)} &\leftarrow \theta^{(N)} - \alpha_{N+1} \nabla g_{\theta^{(N)}}(x), \end{aligned}$$

where  $\alpha_n \in (0, f_{\theta^{(n-1)}}^n(x)/L) \forall n$  and  $\alpha_{N+1} \in (0, 1/L)$ , satisfy both  $l_1(\theta^{(N+1)}) \leq l_1(\theta)$  and  $l_2(\theta^{(N+1)}) \leq l_2(\theta)$ .

**Proof.** As we only consider updates in  $\theta$  for constant  $x$ , we simplify the notation for this proof to  $f^n(\theta) := f_{\theta}^n(x), g(\theta) = g_{\theta}(x)$ . I.e. we have as the two loss terms

$$l_1(\theta) = -\sum_{n=1}^N f^n(\theta) + g(\theta) \quad \text{and} \quad l_2(\theta) = -\sum_{n=1}^N \log f^n(\theta) + g(\theta).$$

In general we have with  $\log f(\theta) < f(\theta)$  that  $l_1(\theta) < l_2(\theta)$ . Similarly we have

$$\nabla l_2(\theta) = -\sum_n \underbrace{\frac{1}{f^n(\theta)}}_{\geq 1} \nabla f^n(\theta) + \nabla g(\theta) \leq -\sum_n \nabla f^n(\theta) + \nabla g(\theta) = \nabla l_1(\theta).$$

Due to the sequential updates we can consider each term separately. For an  $L$ -Lipschitz function  $f^n(\theta)$ , we have that for arbitrary  $x, y$

$$f(y) \leq f(x) + \nabla f(x)^T (y - x) + \frac{L}{2} \|y - x\|_2^2.$$

Choosing  $y = \theta^{(n-1)}$  and  $x = \theta^{(n)} = \theta^{(n-1)} + \alpha_n \nabla \log f^n$  this gives us

$$\begin{aligned} f(\theta^{(n-1)}) &\leq f(\theta^{(n)}) - \frac{\alpha_n}{f^n(\theta^{(n)})} \|\nabla f^n(\theta^{(n)})\|_2^2 + \frac{L\alpha_n^2}{2f^n(\theta^{(n)})^2} \|\nabla f^n(\theta^{(n)})\|_2^2 \\ &= f^n(\theta^{(n)}) - \underbrace{\frac{\alpha_n}{f^n(\theta^{(n)})}}_{\geq 0} \underbrace{\left(1 - \frac{L\alpha_n}{2f^n(\theta^{(n)})}\right)}_{> 0} \|\nabla f^n(\theta^{(n)})\|_2^2 \leq f^n(\theta^{(n)}), \end{aligned}$$

and hence chaining the update steps gives the desired result.  $\square$

That is, updating the terms in  $l_2(\theta)$  sequentially, one can ensure concurrent optimization of  $l_1(\theta)$ . Note that  $l_1(\theta)$  and  $l_2(\theta)$  are not necessarily dual objectives, hence may have different extrema. Nevertheless, a gradient step that decreases one loss also decreases the other with potentially a different magnitude. In practice, we observe this behavior to also hold empirically for joint gradient update steps with shared learning rates. Applying Lemma 2 to the setup in Theorem 2, we establish a useful link between Empirical Bayes and PAC learning.

**Theorem 3 (strong convergence).** *Let  $\mathbf{h}_t^\theta$  be an Itô process as in (2) with drift and diffusion parameters  $\theta = \{\theta_f \cup \theta_G\}$  and its Euler-Maruyama approximation  $\tilde{\mathbf{h}}_t^\theta$  as in (4) for some regular step size  $\Delta t > 0$ . For some coefficient  $R > 0$  and any  $T > 0$ , the inequality below holds*

$$\mathbb{E} \left[ \sup_{0 \leq t \leq T} \left| \mathbb{E}_\theta[\mathbf{h}_t^\theta] - \frac{1}{S} \sum_{s=1}^S \tilde{\mathbf{h}}_t^{\theta^{(s)}} \right| \right] \leq R\Delta t^{1/2},$$

as  $S \rightarrow \infty$ , where  $\{\theta^{(s)} \sim p_\phi(\theta) | s = 1, \dots, S\}$  are i.i.d. draws from a prior  $p_\phi(\theta)$ .

**Proof:** The Euler-Maruyama (EM) approximation converges strongly as

$$\mathbb{E} \left[ |\mathbf{h}_T^\theta - \tilde{\mathbf{h}}_T^\theta| \right] \leq R\Delta t^{1/2},$$

for a positive constant  $R$  and a suitably small step size  $\Delta t$  as discussed e.g. by Kloeden and Platen (2011). To simplify the mathematical notation we follow their approach of comparing the absolute error of the end of the trajectory throughout the proof. As our sampling scheme is unbiased it is a consistent estimator and we have that asymptotically for  $S \rightarrow \infty$

$$\frac{1}{S} \sum_{s=1}^S \tilde{\mathbf{h}}_T^{\theta^{(s)}} = \mathbb{E}_\theta[\tilde{\mathbf{h}}_T^\theta].$$

We then have for the marginal  $\mathbf{h}_T, \tilde{\mathbf{h}}_T$  that

$$\begin{aligned} \mathbb{E} \left[ |\mathbf{h}_T - \tilde{\mathbf{h}}_T| \right] &= \mathbb{E} \left[ |\mathbb{E}_\theta \mathbf{h}_T^\theta - \mathbb{E}_\theta \tilde{\mathbf{h}}_T^\theta| \right] \\ &= \mathbb{E} \left[ \left| \mathbb{E}_\theta \left[ \mathbf{h}_T^\theta - \tilde{\mathbf{h}}_T^\theta \right] \right| \right] \\ &\leq \mathbb{E} \left[ \mathbb{E}_\theta \left[ |\mathbf{h}_T^\theta - \tilde{\mathbf{h}}_T^\theta| \right] \right] \\ &\leq \mathbb{E}_\theta \left[ R\Delta t^{1/2} \right] = R\Delta t^{1/2}, \end{aligned}$$

where the first inequality is due to Jensen and the second due to the strong convergence result for a fixed set of parameters.  $\square$

## C Computational Cost

We present the runtimes of the different approaches in Table 3. D-BNN samples the weights of the neural network directly leading to the runtime term  $\mathcal{O}(MTF)$ . All other approaches do not sample the weights but the linear activations of the each data points leading to  $\mathcal{O}(2MTF)$ . When we apply empirical Bayes, we do not use any regularization term on the weights, while all other approaches contain a penalty term with cost  $\mathcal{O}(W)$ . Using the PAC-framework, we employ a second regularization term that leads to an additional runtime cost of  $\mathcal{O}(TMD^3)$ . However, the cubic cost in  $D$  is invoked by inverting the diffusion matrix  $G_{\theta_G}(h_t, t)$  and can be further reduced by choosing a simpler form for  $G_{\theta_G}(h_t, t)$  (such as diagonal). In case that prior knowledge is available in ODE form, we need to compute the corresponding drift term for each time point and each MC sample leading to the term  $\mathcal{O}(MTP)$ .

## D Further Details on the Experiments

Here we provide the details of the experiment setup we used in obtaining our results reported in the main paper. We observed our results to be robust against most of the design choices.

Table 3: Computational cost analysis in FLOPs for time series of length  $\mathbf{T}$ .  $\mathbf{M}$ : Number of Monte Carlo Samples.  $\mathbf{W}$ : Number of weights in the neural net.  $\mathbf{F}$ : Forward pass cost of a neural net.  $\mathbf{L}$ : Cost for computing the likelihood term.  $\mathbf{D}$ : Number of dimensions.  $\mathbf{P}$ : Cost of a prior SDE integration.

Model	Training per Iteration
D-BNN (SGLD)	$\mathcal{O}(MTF + MTDL + W)$
Variational Bayes	$\mathcal{O}(2MTF + MTDL + W)$
E-Bayes	$\mathcal{O}(2MTF + MTDL)$
E-PAC-Bayes	$\mathcal{O}(2MTF + MTDL + W + TMD^3)$
E-Bayes-Hybrid	$\mathcal{O}(2MTF + MTDL + MTP)$
E-PAC-Bayes-Hybrid	$\mathcal{O}(2MTF + MTDL + W + TMD^3 + MTP)$

### D.1 Lorenz Attractor

We took 200000 Euler-Maruyama steps ahead with a time step size of  $10^{-4}$  and downsampling by factor 0.01, which gives a sequence of 2000 observations with frequency 0.01. We split the first half of this data set into 20 sequences of length 50 and use them for training, and the second half to 10 sequences of length 100 and use for test. For all model variants, we used an Adam optimizer learning rate 0.001, minibatch size of two, a drift net with two hidden layers of 100 neurons and softplus activation function, and a linear diffusion net. The diffusion net models the diagonal entries of the diffusion matrix, while the off-diagonals are set to zero. We trained all models for 100 epochs and observed this training period to be sufficient for convergence. Due to the same reasons as Lotka-Volterra, we did not need to use an observation model also in this experiment and linked the SDE output directly to the likelihood.

### D.2 CMU Motion Capture

In this experiment, we tightly follow the design choices reported in (Yildiz et al., 2019) to maintain commensurateness. This setup assumes the stochastic dynamics are determined in a six-dimensional latent space. Yildiz et al. (2019) use an auto-encoder to map this latent space to the 50-dimensional observation space back and forth. We adopt their exact encoder-decoder architecture and incorporate it into our BNSDE, arriving at the data generating process

$$\begin{aligned}
 \theta_f &\sim p_{\phi_f}(\theta_f), & \theta_G &\sim p_{\phi_G}(\theta_G) \\
 d\mathbf{h}_t | \theta_f, \theta_G &\sim f_{\theta_f}(b_\lambda(\mathbf{h}_t), t)dt + G_{\theta_G}(b_\lambda(\mathbf{h}_t), t)d\beta_t, \\
 \mathbf{z}_t | \mathbf{h}_t &\sim \mathcal{N}(\mathbf{z}_t | a_\psi(\mathbf{h}_t), 0.5 \cdot 10^{-6}\mathbf{I}), \\
 \mathbf{y}_t | \mathbf{z}_t &\sim \mathcal{N}(\mathbf{y}_t | \mathbf{z}_t, 0.5 \cdot 10^{-6}\mathbf{I}), \quad \forall t_k \in \mathbf{t}.
 \end{aligned}$$

Above,  $b_\lambda(\cdot, \cdot)$  is the encoder which takes the observations of the last three time points as input, passes them through two dense layers with 30 neurons and softplus activation function, and then linearly projects them to a six-dimensional latent space, where the dynamics are modeled. The decoder  $a_\psi(\mathbf{h}_t)$  follows the same chain of mapping operations in reverse order. The only difference is that the output layer of the decoder emits only one observation point, as opposed to the encoder admitting three points at once.

We assume a diagonal diffusion matrix, the entries of which are governed by the Bayesian neural net  $G_{\theta_G}(\cdot, \cdot)$  with one hidden layer of 30 neurons, softplus activation function on the hidden layer and the output. The drift function  $f_{\theta_f}(\cdot, \cdot)$  is governed by another separate Bayesian neural net, again with one hidden layer of 30 neurons and softplus activation function on the hidden layer.

We train all models except SGLD with the Adam optimizer for 3000 epochs on seven randomly chosen snippets at a time with a learning rate of  $10^{-3}$ . We use snippet length 30 for the first 1000 epochs, 50 until epoch 2500, and 100 afterwards. SGLD demonstrates significant training instability for this learning rate, hence for it we drop its learning rate to the largest possible stable value  $10^{-5}$  and increase the epoch count to 5000.

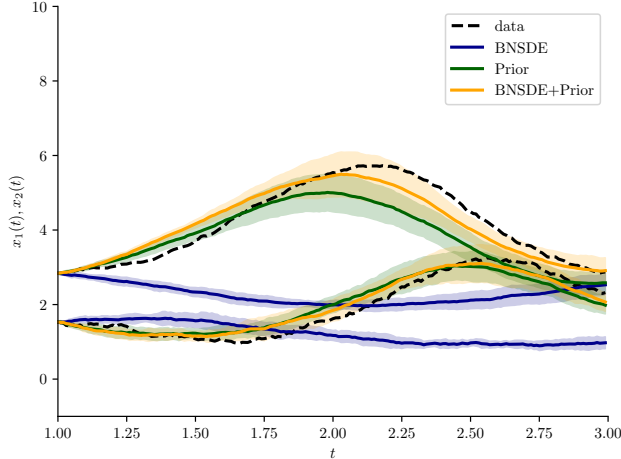


Figure 2: Lotka-Volterra visualization. Error bars indicate three standard deviations over 10 trajectories starting from the true value at  $t = 1$ . The predictions over 200 time steps ( $dt = 0.01$ ) are for: *i*) a BNSDE trained without prior knowledge, *ii*) an SDE with known prior parameters, *iii*) the joint hybrid BNSDE. The dashed lines are the observed trajectories for  $x_t$  and  $y_t$ .

## E Further Experiments

### E.1 Lotka Volterra

We demonstrate the benefits of incorporating prior knowledge although it is a coarse approximation to the true system. We consider the Lotka-Volterra system specified as:

$$\begin{aligned} dx_t &= (\theta_1 x_t - \theta_2 x_t y_t) dt + 0.2 d\beta_t, \\ dy_t &= (-\theta_3 y_t + \theta_4 x_t y_t) dt + 0.3 d\beta_t. \end{aligned}$$

with  $\theta = (2.0, 1.0, 4.0, 1.0)$ . Assuming that the trajectory is observed on the interval  $t = [0, 1]$  with a resolution of  $dt = 0.01$ , we compare the following three methods: *i*) the black-box BNSDE without prior knowledge, *ii*) the white-box SDE in (9) representing partial prior knowledge (parameters are sampled from a normal distribution centered on the true values with a standard deviation of 0.5), and finally *iii*) combining them in our proposed hybrid method. The outcome is summarized in Figure 2. While the plain black-box model delivers a poor fit to data, our hybrid BNSDE brings significant improvement from relevant but inaccurate prior knowledge.

#### E.1.1 Experimental details

We took  $10^5$  Euler-Maruyama steps on the interval  $[0, 10]$  with a time step size of  $10^{-4}$ , downsampling them by a factor of 100 giving us 1000 observations with a frequency of 0.01. We take the first 500 observations on the interval  $[0, 5]$  to be the training data and the observations in  $(5, 10]$  to be the test data. Each sequence is split into ten sequences of length 50. Assuming the diffusion parameters to be known and fixed, both BNSDEs (i.e. with and without prior knowledge) get a 4 layer net as the drift function with 50 neurons per layer and ReLU activation functions. The BNSDE with prior knowledge as well as the raw SDE estimate each get an initial sample of  $\theta$  parameters as the prior information by sampling from a normal distribution centered around the true parameters ( $\tilde{\theta} \sim \mathcal{N}(\tilde{\theta}|\theta, \sigma^2 \mathbf{I}_4)$ ). The models are each trained for 50 epochs with the Adam optimizer and a learning rate of  $1e-3$ . Since both the latent and observed spaces are only two dimensional, we did not need an observation model in this experiment. We directly linked the BNSDE to the likelihood.

### E.2 Lorenz Attractor

As discussed in the main paper, the model is trained solely on the first 1000 observations of a trajectory consisting of 2000 observations, leaving the second half for the test evaluation. Figure 3 visualizes the qualitative difference between the two. Note also the single loop the trajectory performs

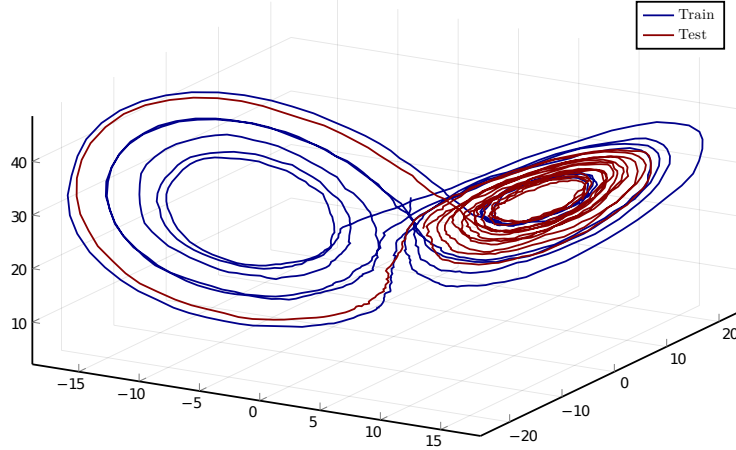
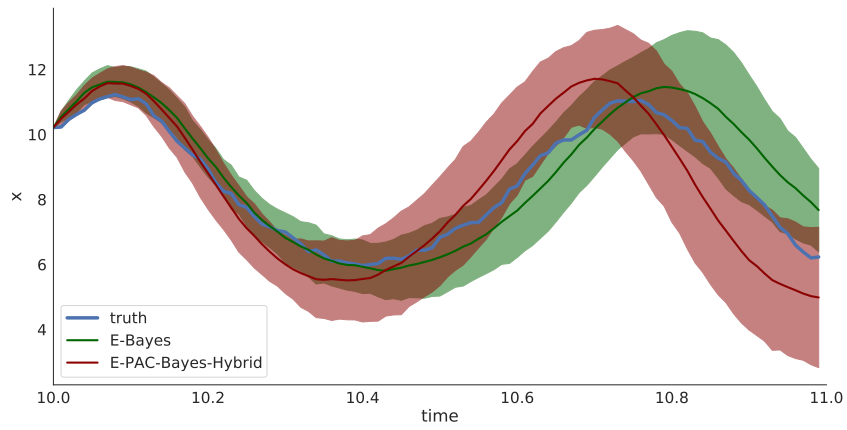


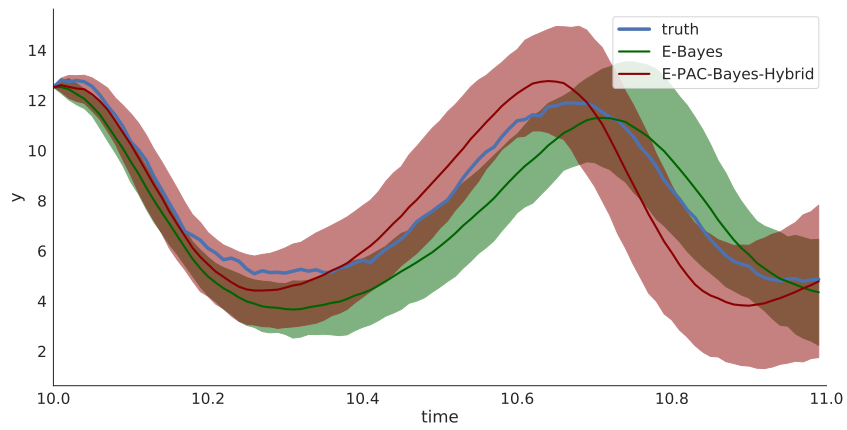
Figure 3: Visualization of the stochastic Lorenz attractor. Of the 2000 observations, the first 1000 constitute the training data (marked in blue), while the second 1000 are the test observations (marked in red). Note the qualitative difference of the two sets.

which we will see again in the 1d projections below. To visualize explore the qualitative difference of our proposed model with weak prior knowledge compared to one lacking this knowledge we consider the situation where we have structural prior knowledge only about  $\rho$  (i.e. the last case in Table 1. In order to properly visualize it we switch from the 3d plot to 1d plots showing always one of the three dimensions vs the time component. We always start at  $T = 10$ , forecasting either 100 steps (as in the numerical evaluation), 200 or 1000 steps. All the following figures show the mean trajectory averaged over 21 trajectories, as well as an envelope of  $\pm 2$  standard deviations. Figure 4 visualizes that at that time scale the qualitative behavior is similar without clear differences. Doubling the predicted time interval as shown in Figure 5 the baseline starts to diverge from the true test sequence, while our proposed model still tracks it closely be it at an increased variance. Finally predicting for 1000 time steps (Figure 6) the chaotic behavior of the Lorenz attractor becomes visible as the mean in both setups no longer tracks the true trajectory. Note however that the baseline keeps has rather small variance and a strong tendency in its predictions that do not replicate the qualitative behavior of the Lorenz attractor. While the proposed model also shows an unreliable average, the large variance, which nearly always includes the true trajectory shows that the qualitative behavior is still replicated properly by individual trajectories of the model. See Figure 7 for seven individual trajectories of each of the two models. All trajectories of *E-PAC-Bayes-Hybrid* show the qualitatively correct behavior, including even the characteristic loop.

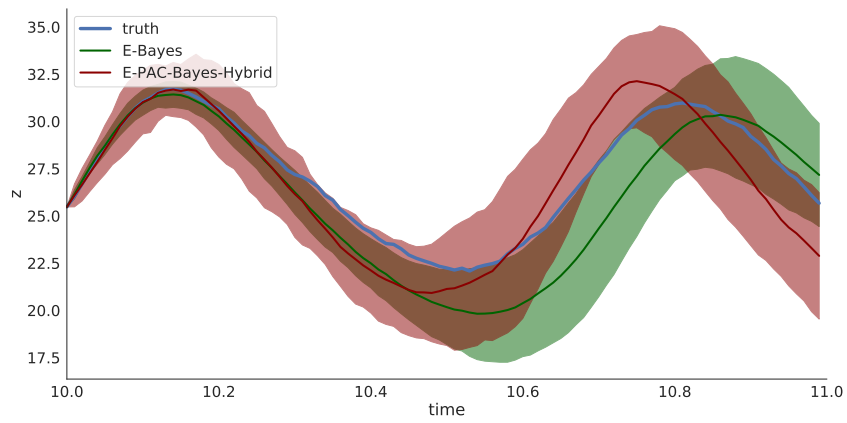




(a)  $x$  coordinate over time

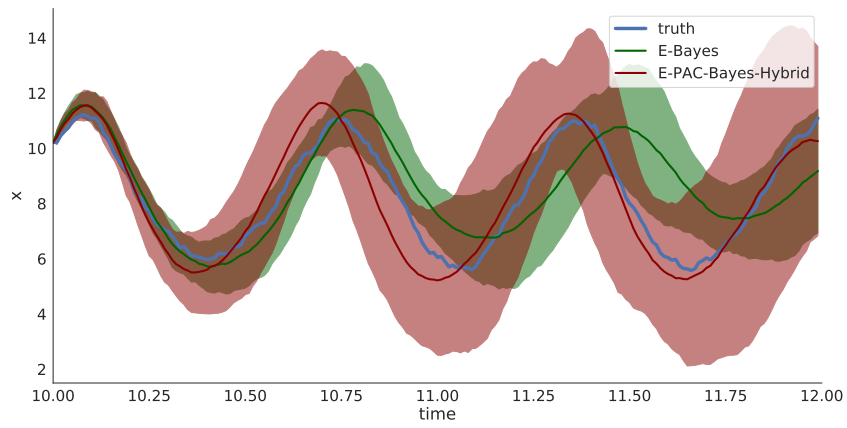


(b)  $y$  coordinate over time

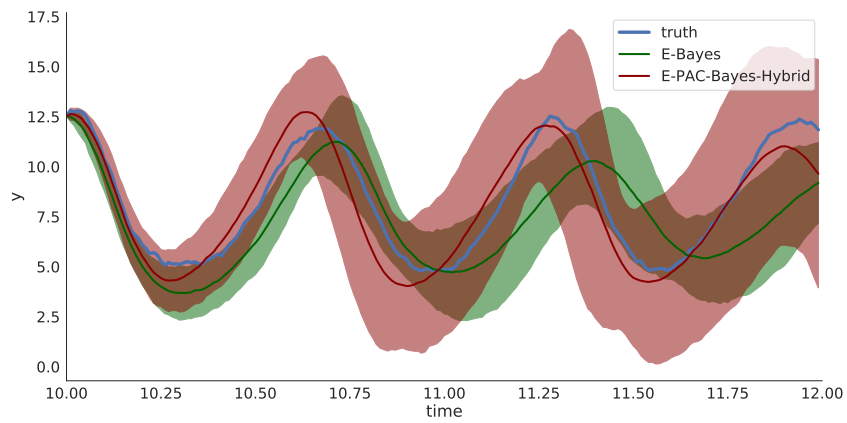


(c)  $z$  coordinate over time

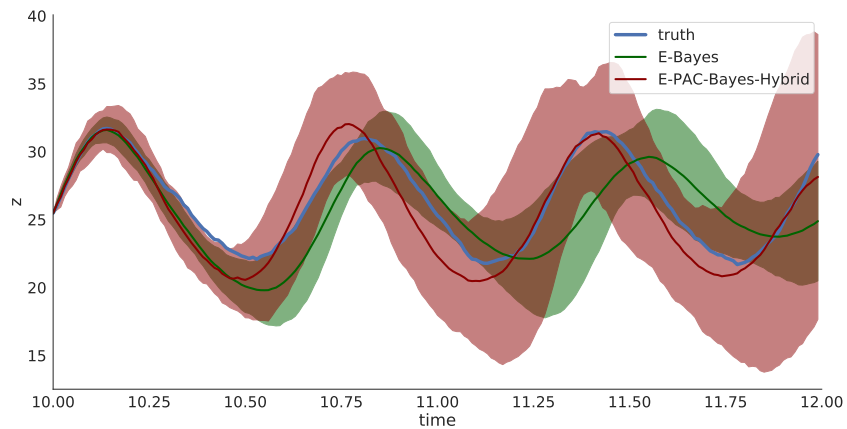
Figure 4: Predicting 100 time steps ahead.



(a)  $x$  coordinate over time

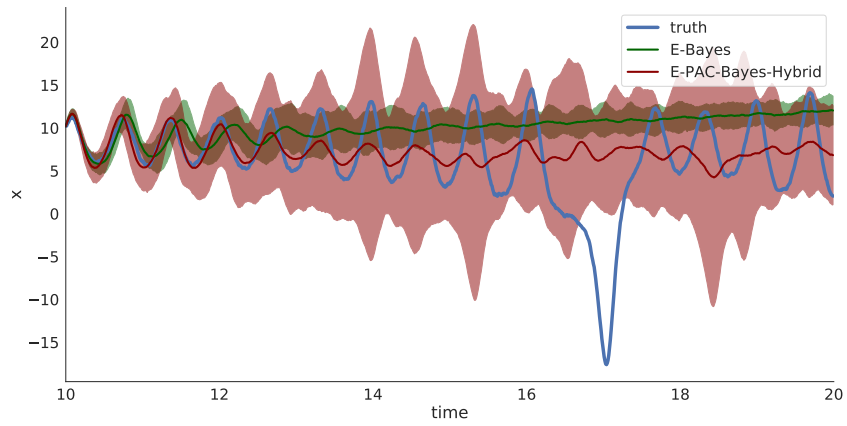


(b)  $y$  coordinate over time

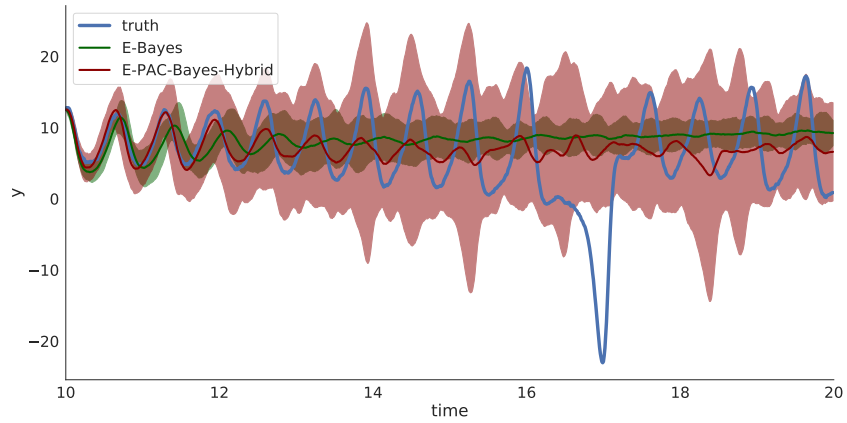


(c)  $z$  coordinate over time

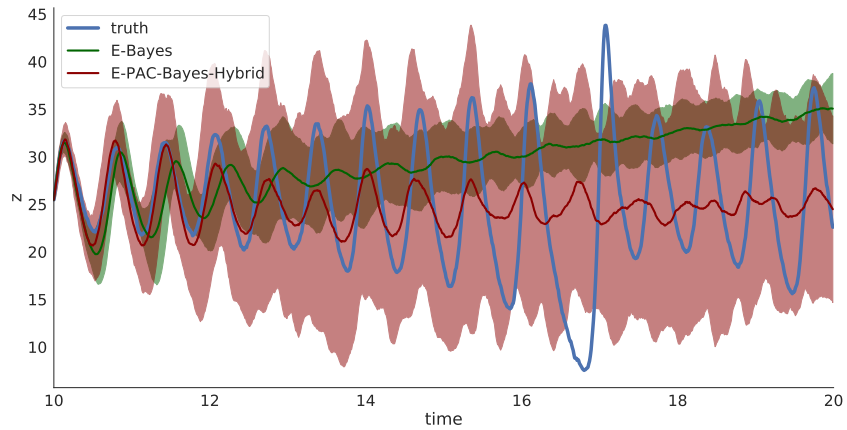
Figure 5: Predicting 200 time steps ahead.



(a)  $x$  coordinate over time

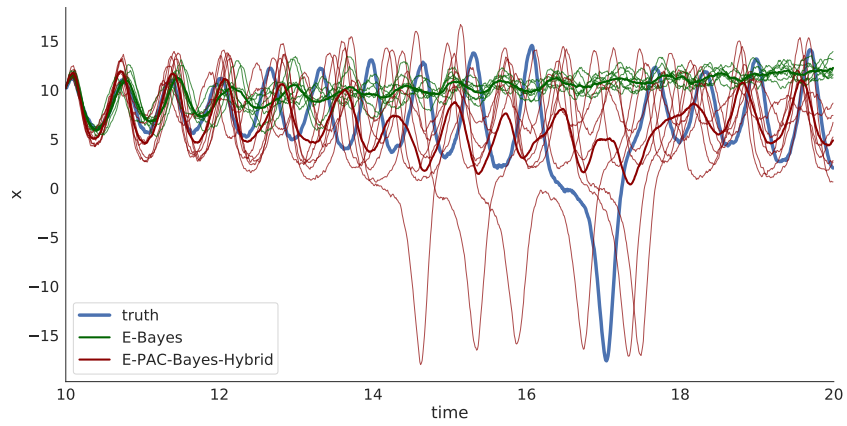


(b)  $y$  coordinate over time

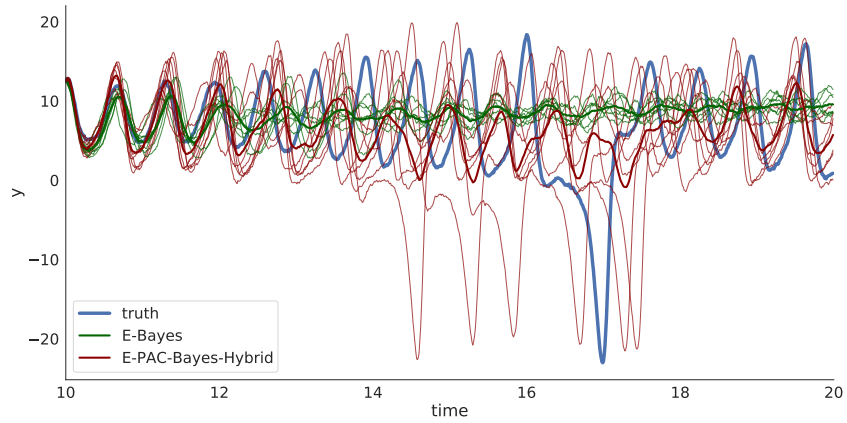


(c)  $z$  coordinate over time

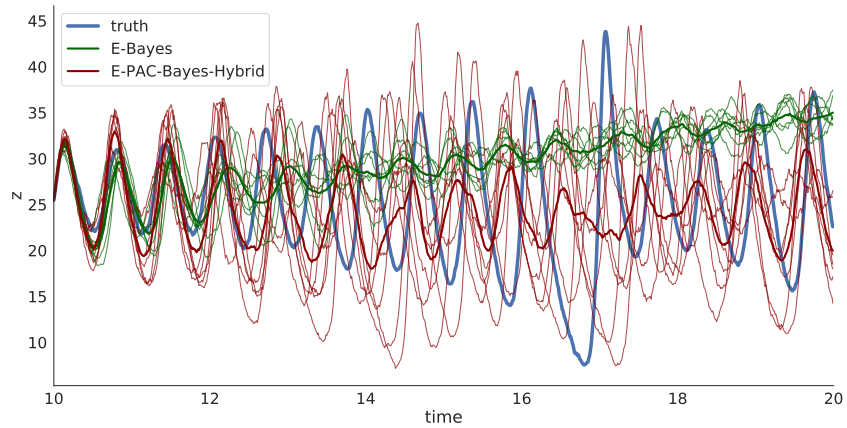
Figure 6: Predicting 1000 time steps ahead.



(a)  $x$  coordinate over time



(b)  $y$  coordinate over time



(c)  $z$  coordinate over time

Figure 7: Predicting 1000 time steps ahead.